Chapter 6
The Importance of Tokyo Bay as a Reservoir for Radioactive Materials Precipitated in the Tokyo Metropolitan Area

Abstract The Tokyo metropolitan area is located in the Kanto Plain, which is found in roughly the center of Japan. The area of high-concentration pollution surrounding Tokyo are the catchments of rivers flowing into Tokyo Bay. Radioactive nuclides deposited there are carried by rainfall and river water and finally flow into Tokyo Bay. That is, Tokyo Bay serves as a reservoir for radioactive nuclides deposited in the Tokyo metropolitan area. Tokyo Bay functions in two ways as a reservoir for radionuclides. One function is to deposit radioactive material that has flowed into Tokyo Bay within sediments and to act as a natural storage facility. The other function is to work as a storage facility for decontaminated radioactive material, which is artificially collected from the land in the metropolitan area. The radioactive materials collected at wastewater treatment facilities in Tokyo are buried as sludge incineration ash at the Central Breakwater under construction in the northwestern part of Tokyo Bay. By the end of 2016, approximately 0.68 TBq of radioactive cesium had been buried in this landfill. In any case, clarifying the behavior of radioactive nuclides in Tokyo Bay is crucial. Therefore, to elucidate the dynamics of radioactive nuclides in the Tokyo metropolitan area, it is necessary to analyze the migration process of radionuclides in these watersheds and their accumulation mechanism in Tokyo Bay. Because the Tokyo metropolitan area has mountains, forests, rural areas, and urban areas, it is difficult to evaluate the routes by which radioactive nuclides deposited on the ground surface flow into Tokyo Bay. However, elucidating the influx processes of radioactive nuclides into Tokyo Bay and the advection, diffusion, and deposition processes into the sediment helps in understanding the role of Tokyo Bay as a reservoir for radioactive nuclides. The revelation of these dynamics is essential information to estimate the future fate of radioactive nuclides deposited in the Tokyo metropolitan area.

Keywords Tokyo Bay · Radioactive cesium · Spatiotemporal change · Sediment · Flux · Inventory · Pollution sources

H. Yamazaki, *Radioactive Contamination of the Tokyo Metropolitan Area*,
https://doi.org/10.1007/978-981-15-7368-2_6

6.1 Introduction

The Tokyo metropolitan area is located in the Kanto Plain, which is found in roughly the center of Japan. The Tokyo metropolitan area administratively includes Tokyo, Kanagawa, Chiba, Saitama, Ibaraki, Tochigi, Gunma, and Yamanashi prefectures. Ibaraki, Tochigi, and Gunma prefectures border Fukushima Prefecture (See Figs. S2.1 and S2.2 in Chap. 2). To the east is the Pacific Ocean, and to the north and west are large forested areas. In the Fukushima disaster, the entire Tokyo metropolitan area was contaminated with radioactive cesium ($^{134+137}$Cs) at approximately 10–300 kBq/m^2 or more, but in the northern part of Chiba Prefecture, approximately 30 km northeast of the center of Tokyo, was particularly contaminated with high concentrations (Fig. 3.2). The highest value shown in Table 3.4 was 881 kBq/m^2. Mountainous forested areas, approximately 100 km farther north, also suffered large-scale radioactive contamination. According to the MEXT airborne monitoring [1], the precipitation of $^{134+137}$Cs in many forested areas may have exceeded 100 kBq/m^2. These areas of high-concentration pollution surrounding Tokyo are the catchments of rivers flowing into Tokyo Bay. Radioactive nuclides deposited there are carried by rainfall and river water and finally flow into Tokyo Bay. That is, Tokyo Bay serves as a reservoir for radioactive nuclides deposited in the Tokyo metropolitan area.

Tokyo Bay is a closed inner bay, but there are many ports, and the bay is congested by navigating ships. In addition, many high-rise buildings have been constructed coastal landfills, and many residents live there. Many factories and commercial facilities are situated along the coast, and approximately ten million people live around Tokyo Bay. If radioactive material from the catchment regions of the Tokyo metropolitan area flows into Tokyo Bay, the radioactive contamination of Tokyo Bay will directly affect the lives of the area residents. Additionally, many inhabitants pursue fishing in this sea since high-quality fish have long been caught in Tokyo Bay.

Tokyo Bay functions in two ways as a reservoir for radionuclides. One function is to deposit radioactive material that has flowed into Tokyo Bay within sediments and to act as a natural storage facility. The other function is to work as a storage facility for decontaminated radioactive material, which is artificially collected from the land in the metropolitan area. As shown in Chap. 5, the radioactive materials collected at wastewater treatment facilities in Tokyo are buried as sludge incineration ash at the Central Breakwater under construction in the northwestern part of Tokyo Bay. By the end of 2016, approximately 0.68 TBq of radioactive cesium had been buried in this landfill.

In any case, clarifying the behavior of radioactive nuclides in Tokyo Bay is crucial. Therefore, to elucidate the dynamics of radioactive nuclides in the Tokyo metropolitan area, it is necessary to analyze the migration process of radionuclides in these watersheds and their accumulation mechanism in Tokyo Bay. Because the Tokyo metropolitan area has mountains, forests, rural areas, and urban areas, it is difficult to evaluate the routes by which radioactive nuclides deposited on the ground surface flow into Tokyo Bay. However, elucidating the influx processes of

radioactive nuclides into Tokyo Bay and the advection, diffusion, and deposition processes into the sediment helps in understanding the role of Tokyo Bay as a reservoir for radioactive nuclides. The revelation of these dynamics is essential information to estimate the future fate of radioactive nuclides deposited in the Tokyo metropolitan area.

Many of the data presented in this chapter have already been published by PLOS ONE in the authors [2].

6.2 Oceanographic Structure of Tokyo Bay

Tokyo Bay is a closed bay 70 km from north to south and 20 km from east to west, with a total area of 1380 km^2 and an average depth of 15 m. It is connected to the Pacific Ocean by the southernmost strait, and its bay mouth is 21 km wide and 700 m deep. The water depth near the Aqua Line shown in Fig. 6.1 is approximately 25–30 m, but the water depth increases rapidly from this point to offshore areas. A submarine valley formed in the center of the strait connects to the open ocean. The closure index determined by the MOE (Ministry of the Environment, Japan) is 1.78 [3]; thus, it is a closed bay where the Japanese Water Pollution Control Law regulates the emissions of nutrients. The closure index is determined as follows: $\{(\sqrt{S}/W) \times (D_1/D_2)\}$, where S is the area of the bay, W is the width of the bay mouth, D_1 is the maximum depth of the bay and D_2 is the depth of the bay mouth. Sea areas with an index of 1.0 or higher are very likely to be eutrophic and are therefore subject to drainage regulations by the MOE. In areas Y and Z shown in Fig. 6.1, DO (dissolved oxygen) in the bottom water is depleted in the summer, and anoxic sea areas appear [4, 5]. The average residence time of seawater varies by season but is reported to be approximately 31 days. Tokyo Bay is closed, but the flow of seawater is complicated. In addition to tidal currents, permanent currents flow throughout the bay, and circular drifts dominate surface water movements: clockwise in winter and counterclockwise in summer [6]. The bottom water moves in a direction opposite to that of the surface water flow. Ocean water from the Pacific flows north down the bottom of the bay until it reaches the innermost part of the bay [4, 5].

Central Tokyo is located on the western side of the bay, surrounded by the metropolitan zones that form the heart of Japan, with a total population of 38 million. The basins of the rivers that flow into Tokyo Bay from the Tokyo metropolitan area occupy a land area of 9100 km^2, and the total amount of flowing river water varies greatly depending on weather conditions, but the average is approximately 1.4×10^7 m^3/day. The principal rivers are the Edogawa, Old Edogawa, Arakawa, Tamagawa, Sumidagawa, and Tsurumigawa rivers [4, 5].

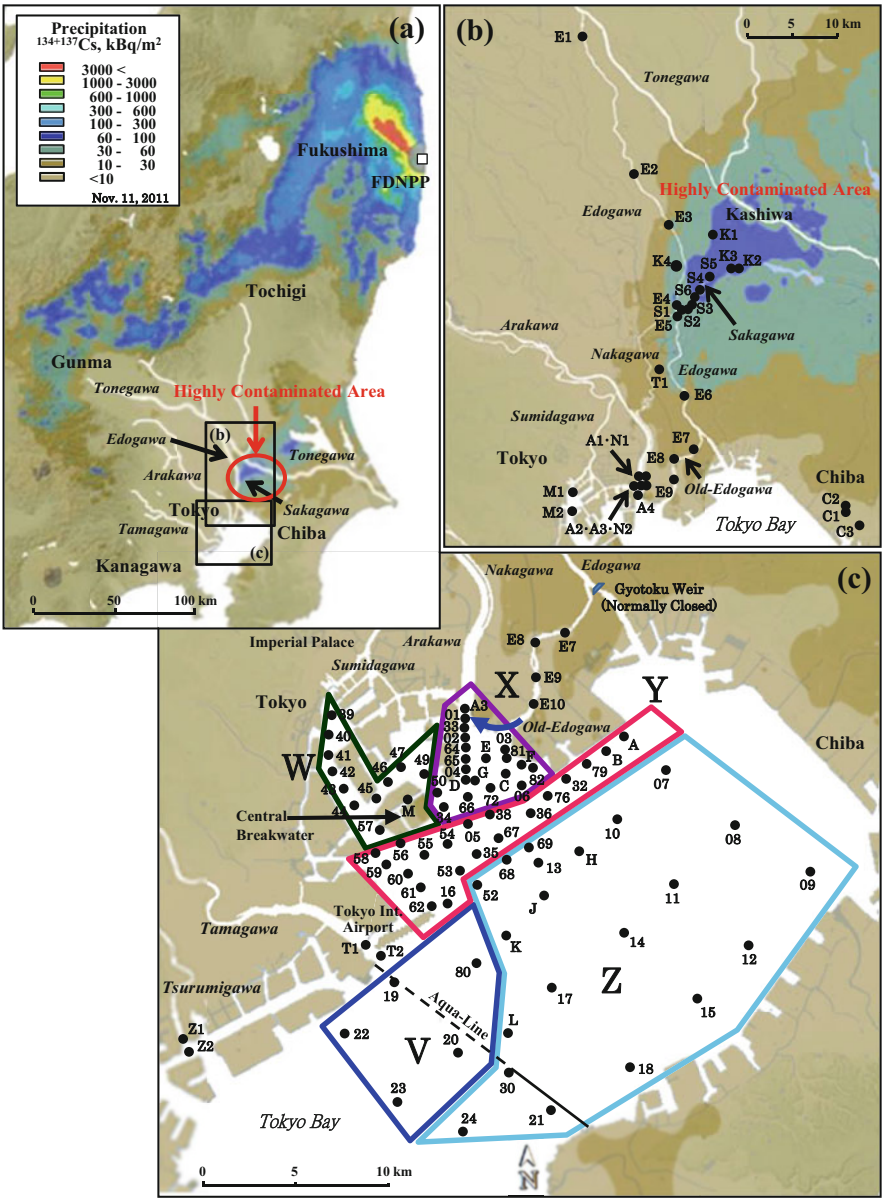

Fig. 6.1 Study areas and sampling sites. Geographic distribution of the radioactive cesium precipitation is quoted from the MEXT airborne monitoring [1]. (**a**) Study area. (**b**) Sampling sites in the Edogawa river system. (**c**) Sampling sites in Tokyo Bay. V: Tamagawa River estuary, W: Sumidagawa River estuary, X: Old Edogawa River estuary, Y: Offshore the Old Edogawa and Sumidagawa estuaries, Z: Central Tokyo Bay. Aqua-Line: Tokyo Bay crossing road. Water in Old Edogawa flows in the direction of the blue arrow in (**c**)

6.3 Status of Radioactive Contamination Around Tokyo Bay and the FDNPP Disaster

The $^{134+137}$Cs pollution map from the airborne monitoring conducted by the MEXT [1] is shown in Fig. 3.2. The results indicate that the catchment area of the Edogawa River was contaminated by 10–100 kBq/m^2 from radioactive cesium discharged in the FDNPP accident. However, the radioactive contamination levels in the catchments of Tokyo Bay's other rivers were lower than those in the catchment of the Edogawa River. Radioactive materials precipitated on the ground surface in the Tokyo metropolitan area are presumably transferred by these rivers until they finally flow into Tokyo Bay, as in the case of artificially discharged environmental contaminants such as heavy metals and pesticides.

Many reports outlining the FDNPP accident have already been released to the public [References 3–8 in Chap. 1]. However, many of these results are analyses of the accident process, whereas few address the environmental radioactive contamination that was caused [1, 7–9]. In particular, after the accident, high-concentration radioactive plumes arrived in the greater Tokyo region, and radionuclides washed out with rainfall on March 16 and 22 in 2011 [10]. Nevertheless, the movement through the greater Tokyo region of radioactive contamination produced by the FDNPP accident has been insufficiently analyzed. Clarifying the movement of environmental radioactive contaminants in the densely populated greater Tokyo region is an important issue related to the problem of low-dose exposure to large populations. Evaluation of the migration processes of radioactive cesium from the Tokyo metropolitan area is also necessary from the viewpoint of reduction and removal of radioactive contamination in these areas. In the author's previous paper [11] and in Chaps. 3 and 5, the behaviors of radioactive contaminants in the soil of the Tokyo metropolitan area are discussed. It is estimated that approximately 5–10% of the radioactive cesium that precipitated into the surface soil migrated via rainfall and rivers in the 5 years after the FDNPP accident (Table 5.3). Perhaps these contaminants flowed into Tokyo Bay.

Before the FDNPP accident, the Chernobyl and Three Mile Island (TMI) accidents affected many people of the world. The TMI is located approximately 150 km west of Washington, D.C., but because it avoided the destruction of the pressure vessel, the emissions of radioactive nuclides to the environment included only rare gas and radioactive iodine nuclides, and the release amount of ^{131}I was estimated to be approximately 0.5 TBq [12, 13]. In the case of the Chernobyl accident, Kyiv City is located 130 km south, and four million residents lived in this metropolitan area. It was reported at the Chernobyl Forum by the IAEA in 2006 [14] that a radioactive plume was transported to Kyiv City by the north wind on May 1, 1986, immediately after the accident. However, regulations on information disclosure were made by the Soviet government at the time, and the actual state and dynamics of radioactive contamination in Kyiv City are hardly understood even at present. Of course, radioactive contamination by the atomic bombs at Hiroshima and Nagasaki is not forgotten. The results of investigations on the environmental dynamics of

radionuclides 60 years after radiation exposure from the atomic bombs have already been reported [15–17]. The greater Tokyo region experienced severe radioactive contamination due to the FDNPP disaster. It was the first time in world history that a densely populated metropolis has undergone massive radioactive contamination.

The study started in August 2011 immediately after the FDNPP accident, with continuous time-series analysis of the distributions and fluctuations of radioactive cesium in sediments and waters in Tokyo Bay and the rivers flowing into Tokyo Bay. Based on the results, the processes of movement from the land and deposition in Tokyo Bay of radioactive cesium that precipitated in the Tokyo metropolitan area after the FDNPP accident were evaluated [2, 11].

Studies on the behavior of radioactive cesium in an urban environment have been performed through simulations [18, 19], but the fluctuation in this radionuclide's spatiotemporal distribution have not been monitored or analyzed over extensive areas for long periods. Numerous studies have reported on the behavior of radioactive materials transported from lakes to lakes and oceans from land contaminated by nuclear disasters such as the Chernobyl and FDNPP accidents. Mixing and depositional processes in the estuary also have significant effects on the dynamics of radionuclides. However, the behavior of cesium as an alkali metal element is often complicated and unknown in estuaries where seawater and river water mix [20–22]. In this chapter, the essential roles that Tokyo Bay and rivers flowing into it play in the movements of radioactive cesium contaminants and the transport and accumulation mechanisms of such contaminants in the greater Tokyo region are clarified.

The NRA (Nuclear Regulation Authority, Japan) has monitored the radioactive contamination derived from the FDNPP accident in the surface sediment of Tokyo Bay since June 2013 [23]. The JCG (Japan Coast Guard) has also been measuring the radioactive contamination of surface sediments in Tokyo Bay since 1981 [24]. Further, survey results of radioactive cesium contamination in the Tokyo Bay area immediately after the accident have been published [25]. However, since their monitoring is spatiotemporally limited, it is insufficient to evaluate the dynamics of radioactive contamination throughout the environments of Tokyo Bay.

6.4 Material and Analytical Methods

6.4.1 Sample Collection

Sediments and waters were sampled in Tokyo Bay and the rivers in its catchment basin. Photograph 6.1 shows a sampling location in Tokyo Bay. Area X is the estuary of the Old Edogawa River very close to the city center. The sampling sites are shown in Fig. 6.1. Sampling was performed at the same sites one to seven times during the study period, which ran from August 20, 2011, to July 12, 2016. Sediment samples were collected at 77 points in Tokyo Bay, ten points in the Edogawa River, and six points in the Sakagawa River. Of the sediment samples collected, 68 were core sediments and 142 were surface sediments. Sediment cores were sampled at

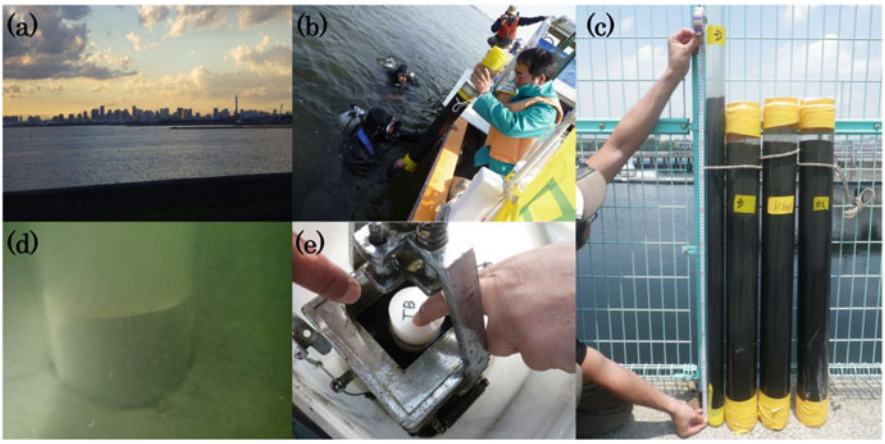

Photo 6.1 Photographs of the landscape in the sampling. (**a**) View of the Tokyo capital from Area X. (**b**) Core sampling by a scuba diver. (**c**) Sediment core was taken from the seafloor. The core sample has a diameter of 10 cm and a maximum length of approximately 90 cm. (**d**) Pull out the acrylic core sampler from the seafloor. (**e**) Surface sediments collected by the Birge-Ekman grab sampler

Site S1 (Fig. 6.1b), where the Sakagawa River flows into the Edogawa River, to evaluate the role of the Sakagawa River in the process of radioactive cesium transport. Soil samples were also collected from the ten sites shown in Fig. 6.1b (K1–K4, S1–S6) for comparison with sediments.

Sediment core sampling was performed using an acrylic pipe with a diameter of 10 cm and a length of 100 cm. The core samples were collected by a diver pushing the pipe into the seabed by hand. Core samples 20–80 cm in length were obtained. Surface sediment specimens were sampled from a boat using a Birge-Ekman bottom grab sampler. Then, on board the boat, after the sediments were recovered, the sediment was inserted into an acrylic pipe with a diameter of 5 cm and a length of 10 cm to obtain samples of the top 5 cm of sediment. Most of the soil and sediment samples consisted of silt and sand with particle sizes of 0.2 mm or less. However, larger pebbles, plant debris, shell fragments, *etc*., were removed with tweezers. Grain size sorting by sieve was not performed. The sediments were pushed out of the pipes, cut into 1 or 2 cm-thick slices in the depth direction, and then thermally dried to a constant weight in a 60 °C oven to remove the water from the sediments. The dried samples were pulverized in an agate mortar, and the radioactivity of the samples was then measured.

Water samples were obtained from the surface of the water by lowering buckets from boats. Divers obtained bottom water from approximately 1 m above the seabed. Without filtering suspended materials out of the water, the radioactive cesium in 20 L of sample water was concentrated using an ammonium phosphomolybdate (AMP) method [26]. After settling overnight, the AMP precipitate was filtered and collected on a membrane filter (pore size 0.8 μm), and the radioactivity of the dried AMP precipitate was then measured. In this way, it was confirmed in a preliminary

experiment that the ionic and suspended radioactive cesium in the sample water could be recovered quantitatively.

6.4.2 Measurement of Radioactivity

The measurement of radioactivity was performed in the same way as described in the other chapters of this book. Radionuclides in the samples were quantified by connecting a 4096-multichannel pulse height analyzer (Lab Equipment, MCA600) to a low-energy HPGe detector (ORTEC, LO-AX/30P) shielded in lead 10 cm thick, sealing the specimens inside a plastic container with a diameter of 5.5 cm and depth of 2.0 cm, and then measuring them via γ-ray spectrometry. The Ge detector calculated the geometric efficiency relative to the sample weight using the American NIST (National Institute of Standards and Technology) Environmental Radioactivity Standards SRM 4350B (river sediment), and SRM 4354 (freshwater lake sediment). The efficiency was corrected to within a range of 2–30 g of the sample weight [27].

The measurement time was set so that the counting error would be less than 5% according to the radioactive intensity of the samples. The nuclides ^{134}Cs (605 keV) and ^{137}Cs (662 keV) were quantified in this study. A ^{134}Cs solution with a known concentration was used to correct the sum peak effect for ^{134}Cs counting. The detection limits of ^{134}Cs and ^{137}Cs under appropriate conditions were 0.6 Bq/kg in sediment samples and 0.3 mBq/L in water samples. Radioactive cesium activity was indicated by the value per sampling day but was corrected for radioactive decay to March 16, 2011, as necessary. In this case, it is denoted as "corrected activity."

6.4.3 Measurements of Heavy Metals and Particle Size Distributions in the Sediments

The heavy metals in the sediments were measured via an XRF method (Rigaku, ZSX-Primus II) using NIST SRM 1646 (estuarine sediment) as the standard sample. The sample measured was prepared from cellulose powder pressed at 0.4 ton/cm^2 in a 4-cm diameter aluminum ring, and 1.2 g of powdered sample was then placed on this disk and repressed at 1.6 ton/cm^2. The correction for the matrix effect was achieved by the X-ray intensity ratio of the peak to the background for each element [28]. Mercury in the sediments was measured by heating vaporization atomic absorption spectrometry (Hiranuma, HG-300).

The particle size distribution of the wet sediment samples was measured using a laser diffractometer (Shimadzu, SALD-3000) with a measurement range of particle sizes from 0.05 to 3000 μm. The dispersion of sedimentary particles was carried out via ultrasonic irradiation (Shimadzu, SUS-200, 42 kHz) using sodium hexametaphosphate as a dispersant. In this paper, the particle size obtained is presented as the volume-based average particle diameter.

6.5 Radioactive Cesium Activity in Water Samples Around Tokyo Bay

It was assumed that radioactive cesium flows into Tokyo Bay through the rivers. Thus, the $^{134+137}$Cs activity of river waters and estuary waters of the major rivers and the seawater of Tokyo Bay were analyzed. The river waters were collected from the surface layer (S), and the seawater was collected at the surface layer (S) and 1 m above the seafloor (B). When water samples were taken at the same site on different days, the radioactive cesium concentration at the site was normalized by weighted averaging of the concentrations corrected for radioactive decay. The results are shown in Table 6.1. The $^{134+137}$Cs activity in water standardized for March 16, 2011, ranges from 4.4 to 178 mBq/L, and in the surface water of the Old Edogawa estuary, it is higher than 20 mBq/L. In particular, higher radioactive cesium activity (39–178 mBq/L) is detected in the river water at the confluence of the Sakagawa and Edogawa rivers (Site S1). In the estuaries of the Sumidagawa and Tamagawa rivers, on the other hand, the cesium activity is mostly lower than 10 mBq/L. The water treatment systems in Tokyo discussed in Chap. 5 are located in the catchments of these rivers. Most of the radioactive cesium deposited on the surface and washed away is believed to be transported to water reclamation centers, not rivers. Therefore, the radioactive cesium concentrations of these rivers are thought to be lower than that of the Edogawa River water system. The radioactive cesium concentrations in the Edogawa River system are mostly somewhat lower than that of seawater (74–78 mBq/L) collected 1.5 km offshore from the FDNPP in September 2013.

The radioactive cesium concentration in the Tokyo Bay water system conforms to the radioactive cesium distribution in the sediments of these areas (Fig. 6.2). Surface and bottom seawaters were sampled from the Old Edogawa estuary to the center of the bay. The ratio of the $^{134+137}$Cs activity in the surface water to that in the bottom water is 2.20 ± 0.85 ($n = 14$), excluding Site J in the center of the bay, showing that the activity was is approximately twofold higher in the surface water than in the bottom water. Most of the analyzed samples were collected from spring to autumn, which is the season when Tokyo Bay seawater is stratifying. The vertical distribution of radioactive cesium in Tokyo Bay indicates that the contaminated river water, which has a low density, diffuses as surface water into the bay because the high-density Pacific seawater penetrates deep into the bay. This distribution implies that radioactive cesium flowed into Tokyo Bay via river water.

Moreover, the radioactivity ratio of ^{134}Cs/^{137}Cs converted to the decay-corrected value immediately after the accident is 0.893 ± 0.025 ($n = 52$). This anomaly is considered to be an appropriate value, as Japanese water samples still contain 1–2 mBq/L of ^{137}Cs as background owing to global fallout from atmospheric nuclear tests [29].

Table 6.1 Radioactive cesium concentrations in water samples collected around Tokyo Bay and offshore the FDNPP

Area	Site	Layer	Sampling date	Detected, mBq/L			Corrected[a], mBq/L				Ratio (S/B)	$^{134}Cs/^{137}Cs$ ratio
				^{134}Cs	^{137}Cs	$^{134+137}Cs$	^{134}Cs	^{137}Cs	$^{134+137}Cs$	Weighted average[b]		
Edogawa River (Upstream)	E4	S	2014/3/24	1.7 ± 1.1	6.2 ± 0.9	7.9 ± 1.5	4.6 ± 3.1	6.7 ± 1.0	11.3 ± 3.3	3.5 ± 0.6		0.688 ± 0.478
			2015/11/11	0.4 ± 0.6	2.6 ± 0.6	2.6 ± 0.6	2.0 ± 2.9	2.8 ± 0.7	2.8 ± 0.7			0.688 ± 1.040
			2016/6/24	0.9 ± 0.5	5.2 ± 0.8	6.1 ± 0.9	5.2 ± 3.1	5.9 ± 0.9	11.1 ± 3.2			0.881 ± 0.544
	E5	S	2016/6/24	1.0 ± 0.4	5.8 ± 0.8	6.8 ± 0.9	6.0 ± 2.5	6.6 ± 0.9	12.5 ± 2.7			0.906 ± 0.402
	E2	S	2014/3/24	4.7 ± 0.9	17.5 ± 1.3	22.2 ± 1.6	13.0 ± 2.6	18.8 ± 1.4	31.7 ± 2.9	18.4 ± 1.9		0.692 ± 0.147
			2016/6/24	0.8 ± 0.4	4.1 ± 0.7	4.9 ± 2.4	4.6 ± 2.3	4.7 ± 0.8	9.3 ± 2.4			0.998 ± 0.520
Sakagawa River	S5	S	2014/4/29	4.2 ± 0.8	12.8 ± 1.4	17.0 ± 1.6	12.1 ± 2.2	13.7 ± 1.5	25.8 ± 2.7			0.880 ± 0.187
	S4	S	2014/4/29	12.2 ± 1.2	38.9 ± 1.4	51.1 ± 1.8	34.9 ± 3.3	41.7 ± 1.5	76.6 ± 3.6			0.836 ± 0.085
	S3	S	2016/6/24	1.8 ± 0.8	10.8 ± 1.0	12.6 ± 1.3	10.6 ± 4.5	12.2 ± 1.1	22.7 ± 4.7			0.866 ± 0.380
	S2	S	2016/6/24	2.7 ± 0.6	17.1 ± 1.2	19.8 ± 1.3	16.0 ± 3.3	19.3 ± 1.3	35.3 ± 3.6			0.829 ± 0.182
	S1	S	2014/4/29	31.3 ± 1.9	82.6 ± 2.4	113.9 ± 3.1	89.5 ± 5.6	88.8 ± 2.5	178.3 ± 6.1	67.2 ± 1.9		1.009 ± 0.069
			2014/3/24	19.2 ± 1.5	48.1 ± 1.8	67.4 ± 2.3	53.2 ± 4.2	51.6 ± 1.9	104.8 ± 4.6			1.032 ± 0.090
			2015/11/12	5.3 ± 0.6	20.7 ± 1.1	26.0 ± 1.3	25.4 ± 3.0	23.0 ± 1.2	48.4 ± 3.3			1.101 ± 0.145
			2016/6/24	3.2 ± 0.5	17.5 ± 1.3	20.7 ± 1.3	18.8 ± 2.7	19.8 ± 1.4	38.6 ± 3.1			0.950 ± 0.154
Edogawa River (Downstream)	E6	S	2016/6/24	0.7 ± 0.5	4.9 ± 0.8	5.5 ± 0.9	4.1 ± 3.1	5.5 ± 0.9	9.5 ± 3.2			0.739 ± 0.568
	E7	S	2016/6/24	0.6 ± 0.5	4.3 ± 0.9	5.0 ± 1.0	3.7 ± 3.1	4.9 ± 1.0	8.6 ± 3.3			0.762 ± 0.658
	E1	S	2014/3/24	2.2 ± 0.6	5.5 ± 0.7	7.7 ± 0.9	6.0 ± 1.5	5.9 ± 0.7	11.9 ± 1.7	14.7 ± 1.6		1.010 ± 0.286
			2016/6/24	2.2 ± 0.6	15.4 ± 1.3	17.6 ± 1.5	12.9 ± 3.7	17.4 ± 1.5	30.3 ± 4.0			0.742 ± 0.225
Old Edogawa River	E3	S	2016/7/12	1.9 ± 0.3	13.8 ± 1.0	15.8 ± 1.1	11.7 ± 1.8	15.6 ± 1.2	27.3 ± 2.1			0.747 ± 0.125
	E10	S	2016/3/24	1.4 ± 0.7	8.3 ± 1.0	9.8 ± 1.2	7.7 ± 3.7	9.4 ± 1.2	17.0 ± 3.9	17.3 ± 2.5		0.817 ± 0.405
			2016/7/12	1.2 ± 0.5	8.9 ± 0.9	10.1 ± 1.1	7.5 ± 3.0	10.0 ± 1.1	17.5 ± 3.2			0.747 ± 0.309
	E11	S	2016/3/24	1.5 ± 0.6	9.9 ± 1.0	11.4 ± 1.1	7.9 ± 3.0	11.1 ± 1.1	19.0 ± 3.2			0.708 ± 0.278

Nakagawa River	N1	S	2016/7/12	1.0 ± 0.4	6.7 ± 0.8	7.7 ± 0.9	5.7 ± 2.5	7.6 ± 0.9	13.3 ± 2.7			0.751 ± 0.343
	N2	S	2016/3/24	2.9 ± 0.5	15.2 ± 1.0	18.1 ± 1.1	15.8 ± 2.5	17.0 ± 1.2	32.8 ± 2.8	21.6 ± 1.8		0.924 ± 0.161
		S	2016/7/12	1.2 ± 0.5	7.9 ± 0.9	9.0 ± 1.1	7.1 ± 3.0	8.9 ± 1.1	16.0 ± 3.2		1.4	0.797 ± 0.355
		B		0.9 ± 0.5	5.6 ± 0.9	6.5 ± 1.0	5.3 ± 3.2	6.4 ± 1.0	11.6 ± 3.3			0.826 ± 0.518
Arakawa River (Estuary)	A1	S	2016/7/12	1.4 ± 0.6	8.8 ± 0.9	10.2 ± 1.1	8.4 ± 3.8	9.9 ± 1.1	18.3 ± 3.9			0.852 ± 0.395
	A2	S	2016/3/24	1.8 ± 0.6	9.7 ± 1.1	11.5 ± 1.3	9.9 ± 3.4	10.9 ± 1.3	20.8 ± 3.6	23.1 ± 2.0		0.915 ± 0.327
		S	2016/7/12	2.3 ± 0.5	12.5 ± 1.1	14.7 ± 1.2	13.6 ± 3.3	14.1 ± 1.2	27.7 ± 3.5		1.3	0.967 ± 0.245
		B		1.5 ± 0.5	10.6 ± 1.1	12.1 ± 1.2	9.2 ± 2.9	11.9 ± 1.2	21.1 ± 3.2			0.771 ± 0.258
	AC	S	2016/3/24	0.9 ± 0.5	6.4 ± 1.1	7.2 ± 1.2	4.9 ± 2.7	7.1 ± 1.2	12.0 ± 2.9	15.8 ± 2.2		0.680 ± 0.391
		S	2016/7/12	1.7 ± 0.7	11.7 ± 1.0	13.3 ± 1.2	9.9 ± 4.2	13.2 ± 1.2	23.1 ± 4.3		1.3	0.750 ± 0.323
		B		1.4 ± 0.8	8.2 ± 1.3	9.6 ± 1.5	8.2 ± 5.1	9.3 ± 1.4	17.5 ± 5.3			0.883 ± 0.564
	A3	S	2016/7/12	2.3 ± 0.6	15.4 ± 0.6	17.7 ± 0.9	13.9 ± 3.9	17.4 ± 0.7	31.3 ± 3.9			0.799 ± 0.224
Old Edogawa River (Estuary)	2	S	2014/3/25	6.8 ± 0.7	15.7 ± 1.2	22.5 ± 1.4	18.7 ± 2.1	16.9 ± 1.2	35.6 ± 2.4	20.9 ± 1.1	1.2	1.109 ± 0.147
		B		4.8 ± 0.8	14.1 ± 1.1	19.0 ± 1.3	13.3 ± 2.3	15.2 ± 1.1	28.5 ± 2.5			0.880 ± 0.163
		S	2015/11/13	1.9 ± 0.5	10.6 ± 0.8	12.5 ± 0.9	8.9 ± 2.5	11.8 ± 0.9	20.7 ± 2.6		2.6	0.752 ± 0.218
		B		0.9 ± 0.4	3.2 ± 0.6	4.1 ± 0.8	4.4 ± 2.0	3.5 ± 0.7	7.9 ± 2.2			1.243 ± 0.629
		S	2016/7/12	2.0 ± 0.6	12.3 ± 1.0	14.3 ± 1.2	11.9 ± 3.8	13.9 ± 1.1	25.8 ± 4.0		2.6	0.859 ± 0.284
		B		0.8 ± 0.5	4.7 ± 0.9	5.5 ± 1.0	4.7 ± 2.8	5.3 ± 1.0	9.9 ± 3.0			0.882 ± 0.562
	64	S	2013/10/4	5.1 ± 0.6	15.3 ± 0.8	20.4 ± 1.0	12.0 ± 1.5	16.3 ± 0.8	28.3 ± 1.7	15.2 ± 1.0	3.8	0.738 ± 0.099
		B		1.3 ± 0.5	4.2 ± 0.6	5.5 ± 0.8	3.0 ± 1.2	4.4 ± 0.6	7.5 ± 1.3			0.687 ± 0.280
	D	S	2013/10/4	4.5 ± 0.8	14.5 ± 1.2	19.0 ± 1.4	10.7 ± 1.9	15.4 ± 1.2	26.0 ± 2.3	13.4 ± 0.7	2.2	0.693 ± 0.138
		B		2.4 ± 0.7	5.9 ± 0.9	8.3 ± 1.1	5.7 ± 1.7	6.3 ± 0.9	12.0 ± 1.9			0.901 ± 0.297
		S	2014/3/25	7.0 ± 1.0	16.8 ± 1.2	23.9 ± 1.6	19.5 ± 2.9	18.0 ± 1.3	37.5 ± 3.1		2.3	1.083 ± 0.177
		B		2.7 ± 0.5	8.3 ± 0.9	11.0 ± 1.0	7.4 ± 1.5	8.9 ± 0.9	16.3 ± 1.8			0.839 ± 0.189
		S	2015/11/13	1.7 ± 0.5	9.5 ± 0.9	11.2 ± 1.0	8.0 ± 2.3	10.6 ± 1.0	18.6 ± 2.5		1.4	0.759 ± 0.230

(continued)

Table 6.1 (continued)

Area	Site	Layer	Sampling date	Detected, mBq/L			Corrected[a], mBq/L				Ratio (S/B)	$^{134}Cs/^{137}Cs$ ratio
				^{134}Cs	^{137}Cs	$^{134+137}Cs$	^{134}Cs	^{137}Cs	$^{134+137}Cs$	Weighted average[b]		
		B		1.2 ± 0.5	6.5 ± 0.8	7.8 ± 0.9	5.9 ± 2.3	7.3 ± 0.9	13.2 ± 2.4			0.815 ± 0.326
		S	2016/7/12	1.8 ± 0.6	9.0 ± 0.9	10.8 ± 1.1	11.0 ± 3.9	10.2 ± 1.0	21.2 ± 4.0		3.3	1.080 ± 0.395
		B		nd	5.7 ± 0.9	5.7 ± 0.9	–	6.4 ± 1.0	6.4 ± 1.0			–
	5	S	2013/10/4	3.3 ± 0.4	8.4 ± 0.8	11.7 ± 0.9	7.8 ± 0.9	8.9 ± 0.9	16.7 ± 1.3	13.0 ± 0.8	1.5	0.872 ± 0.135
		B		2.2 ± 0.3	5.6 ± 0.5	7.8 ± 0.6	5.1 ± 0.8	6.0 ± 0.5	11.1 ± 0.9			0.864 ± 0.150
	38	S	2016/7/12	1.2 ± 0.5	7.1 ± 0.9	8.3 ± 1.1	7.0 ± 3.0	8.0 ± 1.0	15.0 ± 3.2	5.4 ± 0.7	3.1	0.874 ± 0.392
		B		nd	4.3 ± 0.7	4.3 ± 0.7	–	4.8 ± 0.7	4.8 ± 0.7			–
Sumidagawa River	M1	S	2016/3/24	1.4 ± 0.6	6.5 ± 0.8	7.9 ± 1.0	7.9 ± 3.4	7.3 ± 0.9	15.1 ± 3.6			1.083 ± 0.495
	M2	S		0.4 ± 0.7	3.2 ± 0.7	3.6 ± 0.9	2.2 ± 3.7	3.6 ± 0.7	5.8 ± 3.7			0.627 ± 1.037
Tamagawa River	T1	S	2016/3/24	0.3 ± 0.4	2.6 ± 0.7	2.9 ± 0.8	1.6 ± 2.0	2.9 ± 0.8	4.5 ± 2.2			0.544 ± 0.702
	T2	S		0.5 ± 0.6	3.3 ± 0.7	3.8 ± 0.9	2.9 ± 3.2	3.7 ± 0.8	6.6 ± 3.3			0.784 ± 0.877
Tsurumigawa River	Z1	S	2016/3/24	0.6 ± 0.6	3.6 ± 0.9	4.2 ± 1.1	3.4 ± 3.4	4.0 ± 1.0	7.4 ± 3.5			0.851 ± 0.871
	Z2	S		0.6 ± 0.4	4.3 ± 0.7	4.9 ± 0.8	3.4 ± 2.1	4.8 ± 0.8	8.2 ± 2.3			0.720 ± 0.461
Tokyo Bay (Center)	68	S	2014/3/25	4.9 ± 0.5	13.1 ± 1.0	18.0 ± 1.1	13.6 ± 1.3	14.0 ± 1.1	27.6 ± 1.7	15.1 ± 0.9	2.7	0.972 ± 0.120
		B		2.0 ± 0.3	4.3 ± 0.6	6.3 ± 0.7	5.6 ± 0.8	4.6 ± 0.7	10.2 ± 1.1			1.210 ± 0.252
	J	S	2015/11/14	0.5 ± 0.4	1.9 ± 0.5	2.4 ± 0.7	2.3 ± 2.2	2.1 ± 0.6	4.4 ± 2.2	5.4 ± 1.7	0.7	1.075 ± 1.061
		B		0.7 ± 0.5	2.8 ± 0.6	3.5 ± 0.8	3.5 ± 2.4	3.1 ± 0.7	6.6 ± 2.5			1.122 ± 0.795
									Weighted average (n = 52)			0.894 ± 0.025
Offshore the FDNPP[c]	Three sites	S	2013/9/5	17.0 ± 9.0	36.9 ± 19.9	53.9 ± 28.8	39.8 ± 20.6	39.1 ± 21.1	78.0 ± 41.6		1.1	1.018 ± 0.761
		B		16.2 ± 3.1	34.4 ± 7.8	50.6 ± 10.9	37.2 ± 7.1	36.4 ± 8.3	73.7 ± 15.4			1.033 ± 0.304

S: Surface water. B: Bottom water 1 m above the seafloor

[a]Decay-corrected values to March 16, 2011

[b]Calculated using the data excluding the counting errors of more than 30%

[c]Seawaters were collected at three sites 1.5 km offshore the FDNPP. The water depths are 11–16 m

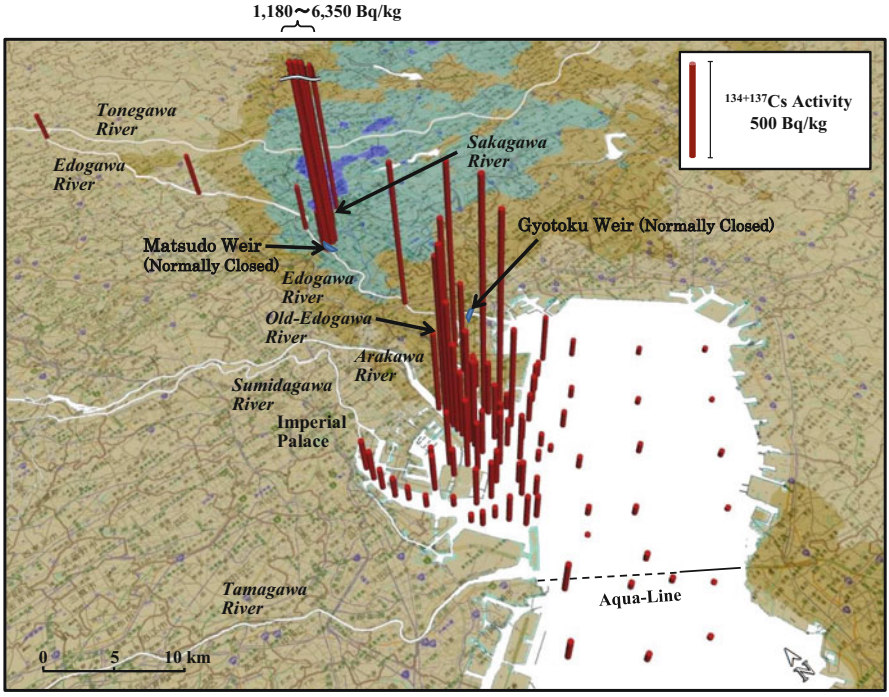

Fig. 6.2 Geographic distributions of $^{134+137}$Cs in the surface sediment in the Tokyo Bay water system. Sediments were collected from August 20, 2011, to July 12, 2016. The $^{134+137}$Cs activities were decay-corrected values to March 16, 2011. The concentrations are shown as an average activity from the surface to 5 cm depth. When there are multiple data at the same site, the concentration expressed as a weighted average value for the counting error

6.6 Spatiotemporal Distribution of Radioactive Cesium in Tokyo Bay Sediments

The measured values obtained from the survey of the Tokyo Bay water system are shown in Table 6.2 (Tokyo Bay) and Table 6.3 (Edogawa Water System). Sampling was performed on different days. Therefore, the radioactive cesium concentrations show values after radioactive decay correction based on March 16, 2011. Multiple measurements collected on different days were subjected to statistical processing. Tables 6.2 and 6.3 show the average activity of $^{134+137}$Cs (sum of ^{134}Cs and ^{137}Cs) in the surface layer of sediments at a depth of 0–5 cm and the inventories of ^{134}Cs, ^{137}Cs, and $^{134+137}$Cs in the sediment cores. The inventory of $^{134+137}$Cs also shows the decay-corrected values based on March 11, 2011. In addition, the average daily flux of $^{134+137}$Cs is shown based on the elapsed time from the accident to sampling. When multiple measurements were taken at the same point, $^{134+137}$Cs radioactivity was evaluated based on the weighted average with counting errors. The deviation of the weighted average was approximated according to the law of uncertainty

Table 6.2 Concentrations, inventories, and fluxes of radioactive cesium in the sediments of Tokyo Bay

Area	Site	Sampling date (n)	Elapsed time[a], day	Contaminated layer[b], cm	Average $^{134+137}$Cs activity of top 5 cm[c, d], Bq/kg	Inventory, kBq/m^2				Flux[e, c], kBq/m^2 day	^{134}Cs/^{137}Cs ratio[c]
						Detected		Corrected			
						^{134}Cs	^{137}Cs	$^{134+137}$Cs	$^{134+137}$Cs	$^{134+137}$Cs	
X	A3	2011 (3)	–	–	416 ± 4	–	–	–	–	–	–
	01	2011–2015 (6)	–	–	810 ± 6	–	–	–	–	–	–
	33	2011 (1)	–	–	873 ± 7	–	–	–	–	–	–
	02	2011–2016 (7)	–	–	647 ± 5	–	–	–		–	–
		2012/11/1	596	12	762 ± 12	8.5	13.9	22.4	29.2	0.049	1.024
		2014/3/25	1105	58	613 ± 32	47.9	142.0	172.0	265.0	0.240	
		2015/11/13	1703	40	253 ± 34	9.0	38.2	47.2	85.9	0.050	
		2016/7/12	1945	52	352 ± 23	14.0	74.7	88.7	168.4	0.086	0.995
	64	2012–2015 (4)	–	–	470 ± 7	–	–	–	–	–	–
		2013/10/4	933	26	371 ± 12	11.2	24.7	35.9	52.6	0.056	1.009
	65	2012–2015 (5)	–	–	355 ± 6	–	–	–	–	–	–
	04	2011 (2)	–	–	593 ± 8	–	–	–	–	–	–
	D	2011–2016 (7)	–	–	466 ± 5	–	–	–	–	–	–
		2011/8/20	157	26	388 ± 11	9.3	10.8	20.1	21.7	0.138	0.981
		2012/4/2	383	26	509 ± 11	12.1	17.4	29.4	35.0	0.091	0.989
		2012/11/1	596	44	721 ± 17	21.1	34.8	55.8	72.6	0.122	1.014
		2013/10/4	933	44	471 ± 11	17.7	39.2	56.9	83.4	0.089	1.007
		2014/3/25	1105	42	465 ± 13	17.2	44.2	61.5	95.1	0.086	1.008

		2015/11/13	1703	70	366 ± 17	18.0	76.3	94.3	171.0	0.100	1.018
		2016/7/12	1945	78	379 ± 18	16.9	87.1	104.0	200.0	0.103	1.029
	G	2016/7/12	1945	70	345 ± 19	15.0	78.5	93.5	178.9	0.092	1.013
	50	2012 (1)	–	–	377 ± 11	–	–	–	–	–	–
	34	2011–2012 (2)	–	–	271 ± 6	–	–	–	–	–	–
		2012/11/1	596	18	297 ± 9	2.0	3.3	5.3	6.9	0.012	0.969
	66	2012–2015 (4)	–	–	245 ± 6	–	–	–	–	–	–
	72	2012/11/1	596	16	306 ± 8	2.1	3.4	5.5	7.1	0.012	0.964
	03	2011 (2)	–	–	1085 ± 9	–	–	–	–	–	–
		2012/4/2	383	36	207 ± 17[f]	53.0	72.8	126.0	150.1	0.392	1.011
		2012/11/1	596	18	126 ± 7[g]	6.4	10.8	17.2	22.3	0.037	0.968
	E	2015 (1)	–	–	398 ± 21	–	–	–	–	–	–
	81	2014 (1)	–	–	282 ± 6	–	–	–	–	–	–
	F	2012 (2)	–	–	959 ± 18	–	–	–	–	–	–
	C	2011–2014 (4)	–	–	140 ± 4	–	–	–	–	–	–
		2011/8/20	157	10	256 ± 11	2.7	3.1	5.8	6.2	0.041	0.972
		2012/4/2	383	16	465 ± 30	4.3	6.1	10.4	12.4	0.032	0.995
		2012/11/1	596	20	115 ± 7	1.4	2.3	3.7	4.8	0.008	1.015
		2014/3/25	1105	10	104 ± 7	0.6	1.5	2.1	3.3	0.003	1.139
	06	2011–2012 (3)	–	–	414 ± 9	–	–	–	–	–	–
		2012/11/1	596	8	124 ± 8	0.6	1.1	1.8	2.3	0.004	0.823
	82	2014 (1)	–	–	78 ± 7	–	–	–	–	–	–

(continued)

Table 6.2 (continued)

Area	Site	Sampling date (n)	Elapsed time[a], day	Contaminated layer[b], cm	Average $^{134+137}$Cs activity of top 5 cm[c, d], Bq/kg	Inventory, kBq/m^2				Flux[e, c], kBq/m^2 day	^{134}Cs/^{137}Cs ratio[c]
						Detected		Corrected			
						^{134}Cs	^{137}Cs	^{134}+^{137}Cs	^{134}+^{137}Cs	$^{134+137}$Cs	
Y	05	2011–2014 (5)	–	–	296 ± 4	–	–	–	–	–	–
		2013/10/4	933	30	278 ± 15	2.4	5.4	7.8	11.4	0.012	0.969
	38	2012–2015 (4)	–	–	147 ± 5	–	–	–	–	–	–
		2012/4/2	383	26	209 ± 11	2.3	3.1	5.3	6.3	0.016	0.982
		2012/11/1	596	16	147 ± 13	0.7	1.1	1.8	2.4	0.004	
		2014/3/25	1105	28	141 ± 11	1.9	4.8	6.7	10.3	0.009	1.025
	54	2012–2014 (2)	–	–	189 ± 7	–	–	–	–	–	–
		2012/11/1	596	28	226 ± 11	1.8	3.0	4.7	6.1	0.010	0.960
	55	2012 (1)	–	–	214 ± 12	–	–	–	–	–	–
	53	2012 (1)	–	–	195 ± 7	–	–	–	–	–	–
	35	2011 (1)	–	–	106 ± 6	–	–	–	–	–	–
	67	2012 (1)	–	–	254 ± 10	–	–	–	–	–	–
	36	2011–2015 (4)	–	–	95 ± 4	–	–	–	–	–	–
		2014/3/25	1105	10	119 ± 9	0.4	0.9	1.3	2.1	0.002	1.059
	76	2012–2014 (2)	–	–	149 ± 6	–	–	–	–	–	–
	32	2011–2015 (4)	–	–	136 ± 3	–	–	–	–	–	–
		2012/11/1	596	18	304 ± 9	3.4	5.6	9.0	11.7	0.020	1.006
	79	2012 (2)	–	–	146 ± 8	–	–	–	–	–	–

		2012/11/1	596	18	158 ± 11	1.1	1.9	2.9	3.8	0.006	1.009
	B	2011/8/20	157	16	69 ± 6	2.5	2.8	5.3	5.8	0.037	0.958
	A	2011–2012 (3)	–	–	233 ± 6	–	–	–	–	–	–
		2011/8/20	157	6	71 ± 9	0.3	0.3	0.6	0.7	0.004	0.959
		2012/11/1	596	36	289 ± 12	4.1	6.9	11.1	14.4	0.024	0.992
	16	2011–2015 (3)	–	–	126 ± 3	–	–	–	–	–	–
	62	2012 (1)	–	–	176 ± 7	–	–	–	–	–	–
	61	2012/11/1	596	16	149 ± 7	2.0	3.4	5.3	6.9	0.012	0.949
	60	2012–2014 (2)	–	–	57 ± 3	–	–	–	–	–	–
	59	2012/11/1	596	16	80 ± 5	1.3	2.2	3.5	4.6	0.008	0.984
	56	2012–2014 (2)	–	–	124 ± 11	–	–	–	–	–	–
	58	2012 (1)	–	–	40 ± 3	–	–	–	–	–	–
W	57	2012–2014 (2)	–	–	48 ± 3	–	–	–	–	–	–
		2012/11/1	596	24	56 ± 4	1.0	1.6	2.7	3.5	0.006	1.075
	44	2012 (1)	–	–	62 ± 4	–	–	–	–	–	–
	43	2012/11/1	596	22	72 ± 6	1.5	2.6	4.0	5.2	0.009	1.017
	42	2012 (1)	–	–	107 ± 4	–	–	–	–	–	–
	41	2012/11/1	596	22	113 ± 7	1.9	3.2	5.1	6.6	0.011	0.967
	40	2012 (1)	–	–	165 ± 7	–	–	–	–	–	–
	39	2012 (1)	–	–	167 ± 7	–	–	–	–	–	–
	45	2012/11/1	596	10	205 ± 9	1.9	3.2	5.1	6.6	0.011	0.955
	46	2012–2014 (2)	–	–	174 ± 6	–	–	–	–	–	–

(continued)

Table 6.2 (continued)

Area	Site	Sampling date (n)	Elapsed time[a], day	Contaminated layer[b], cm	Average $^{134+137}$Cs activity of top 5 cm[c, d], Bq/kg	Inventory, kBq/m^2				Flux[e, c], kBq/m^2 day	^{134}Cs/^{137}Cs ratio[c]
						Detected		Corrected			
						^{134}Cs	^{137}Cs	$^{134+137}$Cs	$^{134+137}$Cs	$^{134+137}$Cs	
	47	2012 (1)	–	–	59 ± 4	–	–	–	–	–	–
	M	2012–2014 (2)	–	–	155 ± 5	–	–	–	–	–	–
	49	2012–2015 (3)	–	–	304 ± 8	–	–	–	–	–	–
		2012/11/1	596	26	336 ± 18	5.3	9.0	14.3	18.5	0.031	0.983
		2015/11/13	1703	4	36 ± 8	0.1	0.4	0.5	1.0	0.001	1.176
Z	52	2012/11/1	596	14	140 ± 11	0.7	1.2	1.9	2.5	0.004	0.993
		2014/3/25	1105	5	57 ± 12	0.2	0.5	0.7	1.1	0.001	0.859
		2015/11/13	1703	<5	60 ± 12	0.1	0.3	0.4	0.7	0.000	0.868
	68	2012–2015 (3)	–	–	50 ± 4	–	–	–	–	–	–
		2012/11/1	596	6	35 ± 5	0.1	0.2	0.4	0.5	0.001	0.801
		2014/3/25	1105	16	99 ± 19	0.4	1.0	1.5	2.3	0.002	0.968
		2015/11/13	1703	20	104 ± 18	0.5	2.5	2.8	5.0	0.003	0.984
	69	2012/11/1	596	<5	115 ± 4	0.3	0.6	1.0	1.3	0.002	0.907
		2014/3/25	1105	2.5	19 ± 3	0.0	0.3	0.3	0.4	0.000	0.540
	13	2011/10/1	199	<5	91 ± 4	0.3	0.4	0.7	0.8	0.004	0.987
		2011/12/3	262	<5	11 ± 2	0.1	0.1	0.2	0.3	0.001	0.834
		2014/3/25	1105	2.5	22 ± 4	0.1	0.3	0.4	0.5	0.000	0.791

		2015/11/13	1703	<5	22 ± 6	0.0	0.1	0.1	0.2	0.000	0.914
	J	2015/11/13	1703	8	59 ± 8	0.1	0.4	0.4	0.8	0.000	1.141
	K	2015/11/13	1703	<5	42 ± 8	0.0	0.1	0.2	0.3	0.000	1.258
	H	2015/11/13	1703	<5	81 ± 11	0.1	0.4	0.5	0.9	0.001	1.074
	10	2011/10/1	199	<5	57 ± 3	0.2	0.3	0.5	0.6	0.003	1.005
		2011/12/3	262	<5	62 ± 3	0.5	0.7	1.3	1.4	0.005	0.833
		2014/3/25	1105	2.5	38 ± 8	0.1	0.5	0.6	0.9	0.001	1.062
		2015/11/13	1703	<5	25 ± 5	0.0	0.1	0.2	0.3	0.000	1.811
	07	2011/10/1	199	<5	53 ± 2	0.3	0.5	0.8	0.9	0.005	0.825
		2011/12/3	262	<5	162 ± 3	2.4	3.0	5.4	6.1	0.023	1.003
		2014/3/25	1105	5	56 ± 11	0.3	0.9	1.2	1.7	0.002	0.900
		2015/11/13	1703	<5	32 ± 4	0.1	0.3	0.4	0.7	0.000	1.040
	08	2011/10/1	199	<5	22 ± 2	0.1	0.1	0.2	0.3	0.004	0.890
		2011/12/3	262	<5	45 ± 3	0.5	0.6	1.1	1.2	0.005	0.999
		2014/3/25	1105	5	57 ± 11	0.2	0.7	0.9	1.4	0.001	0.930
	11	2011/10/1	199	<5	26 ± 3	0.0	0.2	0.2	0.2	0.001	0.218
		2011/12/3	262	<5	11 ± 2	0.1	0.1	0.2	0.3	0.001	1.385
		2014/3/25	1105	2.5	56 ± 9	0.2	0.5	0.7	1.0	0.001	0.991
		2015/11/13	1703	<5	46 ± 10	0.0	0.2	0.2	0.4	0.000	0.957
	14	2011/10/1	199	<5	52 ± 4	0.2	0.2	0.4	0.5	0.002	1.002
		2011/12/3	262	<5	52 ± 3	0.4	0.4	0.8	0.9	0.003	1.309
		2014/3/25	1105	2.5	19 ± 9	0.0	0.2	0.3	0.4	0.000	1.187
	17	2011/10/1	199	<5	50 ± 3	0.2	0.3	0.5	0.6	0.003	0.989
		2011/12/3	262	<5	46 ± 3	0.3	0.5	0.9	1.0	0.004	0.790
		2014/3/25	1105	2.5	34 ± 9	0.1	0.4	0.5	0.7	0.001	0.874
		2015/11/13	1703	<5	26 ± 5	0.0	0.1	0.1	0.2	0.000	1.283

(continued)

Table 6.2 (continued)

Area	Site	Sampling date (n)	Elapsed time[a], day	Contaminated layer[b], cm	Average $^{134+137}$Cs activity of top 5 cm[c, d], Bq/kg	Inventory, kBq/m^2				Flux[e, c], kBq/m^2 day	^{134}Cs/^{137}Cs ratio[c]
						Detected		Corrected			
						^{134}Cs	^{137}Cs	$^{134+137}$Cs	$^{134+137}$Cs	$^{134+137}$Cs	
	09	2011/10/1	199	<5	38 ± 3	0.2	0.3	0.5	0.6	0.003	0.920
		2014/3/25	1105	–	7 ± 2	0.0	2.1	0.2	0.2	0.000	–
	12	2011/10/1	199	–	2 ± 1	0.0	0.0	0.0	0.0	0.000	–
		2014/3/25	1105	2.5	31 ± 7	0.1	0.2	0.3	0.5	0.001	0.941
	15	2011/10/1	199	<5	22 ± 2	0.1	0.2	0.3	0.3	0.002	0.910
		2014/3/25	1105	5	37 ± 11	0.1	0.4	0.5	0.8	0.001	0.960
	18	2011/10/1	199	<5	11 ± 1	0.4	0.4	0.8	0.9	0.004	1.211
		2014/3/25	1105	–	2 ± 1	0.0	0.1	0.1	0.1	0.000	–
	L	2015/11/13	1703	<5	36 ± 5	0.0	0.2	0.3	0.5	0.000	1.045
	30	2011/10/1	199	<5	22 ± 2	0.2	0.2	0.5	0.5	0.003	1.071
	21	2011/10/1	199	<5	10 ± 1	0.2	0.4	0.6	0.6	0.003	0.712
		2014/3/25	1105	–	1 ± 1	0.0	0.0	0.0	0.0	0.000	–
	24	2011/10/1	199	–	10 ± 1	0.0	0.1	0.1	0.2	0.001	–
V	19	2011/10/1	199	<5	136 ± 5	1.0	1.2	2.2	2.4	0.012	1.024
		2011/12/3	262	<5	234 ± 6	4.2	4.4	9.7	11.0	0.042	0.962
	22	2011/10/1	199	<5	118 ± 5	0.5	0.6	1.1	1.2	0.006	1.003
	23	2011/10/1	199	<5	42 ± 3	0.2	0.3	0.5	0.5	0.003	0.754

	20	2011/10/1	199	<5	48 ± 3	0.1	0.3	0.5	0.5	0.003	0.517
		2011/12/3	262	<5	75 ± 5	0.6	0.8	1.4	1.6	0.006	0.995
		2014/3/25	1105	–	3 ± 1	0.0	0.2	0.2	0.2	0.000	–
	80	2014/3/25	1105	–	nd	0.0	0.0	0.0	0.0	0.000	–
								Weighted average[h] (n = 117)			1.006 ± 0.003

Values in parentheses are the number of sampling
[a]Elapsed time is from March 16, 2011, to the sampling date
[b]Contaminated layer means the thickness from the surface to the deepest layer where ^{134}Cs is detected
[c]Calculated using the decay-corrected value to March 16, 2011
[d]Weighted average value for multiple samples
[e]Calculated using inventory and elapsed time
[f]The concentration maximum appeared under the 5 cm depth
[g]The peak of radioactive cesium disappeared
[h]Value for the counting error within 5%. Data not listed in this table also included in the calculation

Table 6.3 Concentrations, inventories, and fluxes of radioactive cesium in the sediment of the Edogawa and Sakagawa rivers

Area	Site	Sampling date	Elapsed time[a], day	Contaminated layer[b], cm	$^{134+137}$Cs activity of top 5 cm[c, d], Bq/kg	Inventory[c], kBq/m^2			Flux[c, e], kBq/m^2 day	^{134}Cs/^{137}Cs ratio[c]
						^{134}Cs	^{137}Cs	$^{134+137}$Cs	$^{134+137}$Cs	
Edogawa River (Upstream)	E1	2011/12/3	262	<5	120 ± 2	4.4	4.3	8.7	0.033	1.039
		2015/11/11	1701	25		107	107	214	0.126	1.005
	E2	2011/12/3	262	<5	203 ± 3	7.8	7.7	15.5	0.060	1.031
		2015/11/12	1702	15		12.0	11.7	23.7	0.014	1.012
	E3	2011/12/3	262	<5	222 ± 4	19.5	18.8	38.3	0.146	1.036
		2015/11/12	1702	5		1.4	1.6	3.0	0.002	1.027
	E4	2011/12/3	262	<5	199 ± 4	15.4	15.5	30.9	0.118	0.998
		2015/11/12	1702	24		8.1	7.9	16.0	0.010	1.026
Sakagawa River (A tributary to Edogawa River)	S5	2014/4/29	1140	13	4160 ± 40	339	336	675	0.592	1.009
	S4	2014/4/29	1140	14	1180 ± 11	98.0	98	196	0.172	0.996
	S6	2014/4/29	1140	41	1310 ± 22	460	449	909	0.797	1.023
	S3	2014/4/29	1140	5	1810 ± 14	70.0	70.4	140	0.123	0.994
	S2	2014/4/29	1140	14	5230 ± 46	152	152	303	0.440	1.001
	S1	2014/4/29	1140	50	6350 ± 64	571	565	1140	0.997	1.011
		2015/11/13	63 (1703)[f]	12	3020 ± 44	33.1	32.8	65.9	1.030	1.012
		2016/6/25	288 (1928)[f]	32	3630 ± 67	145	141	285	0.993	1.029

Edogawa River (Downstream)	E5	2011/12/3	262	<5	581 ± 8	13.6	13.4	27.0	0.103	1.023
		2014/3/24	1104	<5		44.0	43.3	87.3	0.079	1.036
		2015/11/12	1702	20		7.7	8.1	15.8	0.009	0.959
	E6	2011/12/3	262	<5	697 ± 6	35.0	34.6	69.6	0.266	1.000
		2015/11/12	1702	31.5		141	141	282	0.166	1.003
	E7	2011/12/3	262	<5	881 ± 10	30.3	32.0	62.3	0.238	0.947
		2014/3/24	1104	<5		6.9	6.8	13.7	0.012	1.027
	E8	2012/4/3	384	<5	706 ± 17	11.8	11.4	23.2	0.060	1.038
	E9	2012/4/3	384	<5	464 ± 10	11.8	11.9	23.7	0.062	1.000
	E10	2012/4/3	384	<5	133 ± 5	4.4	4.7	9.1	0.024	0.949
									Average[d]	1.009 ± 0.025

[a]Elapsed time is from March 16, 2011, to the sampling date
[b]Contaminated layer means the thickness from the surface to the deepest layer where ^{134}Cs is detected
[c]Calculated using the decay-corrected value to March 16, 2011
[d]Weighted average value for multiple samples
[e]Calculated using inventory and elapsed time
[f]The sediments deposited after the flood on September 11, 2015

propagation. The radioactivity ratio of ^{134}Cs and ^{137}Cs based on March 16, 2011, was also calculated to ensure the reliability of the analysis. The ^{134}Cs/^{137}Cs activity ratio immediately after the accident is believed to have been almost 1.0 [30–32]. Figure 6.2 shows the geographic distribution of the average concentration of $^{134+137}$Cs at each sediment sampling site in the Tokyo Bay water system.

6.6.1 *Distribution of Radioactive Cesium in the Surface Sediments of Tokyo Bay*

The highest $^{134+137}$Cs concentration of all measurements in Tokyo Bay was 1340 ± 13 Bq/kg found in surface sediments (0–5 cm) sampled on November 1, 2012, at Site 01 in the Old Edogawa estuary. Six samplings were performed at the site between October 1, 2011, and November 13, 2015. These $^{134+137}$Cs concentrations tended to decrease over time, but the water depth was as shallow as approximately 5 m, and the river water from the Old Edogawa flowed in, so their concentrations and vertical distributions were greatly affected. The weighted average concentration of $^{134+137}$Cs during the whole monitoring period was 810 ± 6 Bq/kg. Since an anoxic water mass is dominant in the inner part of Tokyo Bay [4, 5], the sediment is not affected much by the activity of benthic organisms. However, this estuary not only shallow is but also hosts navigation of many vessels, and the sediment is highly likely to undergo physical mixing. Therefore, divers visually inspected the seafloor and collected sediments that appeared not to be disturbed. However, it was challenging to collect a stable sedimentary layer from the same place each time.

The $^{134+137}$Cs concentrations in the surface sediments of Tokyo Bay were high in the estuary where the Arakawa and Old Edogawa rivers flow in but low in the central part of the bay. As shown in Fig. 6.1, depending on the $^{134+137}$Cs concentration and the characteristics of the water mass, the contaminated sediments in the Tokyo Bay sea areas can be classified into V (the Tamagawa River estuary), W (the Sumidagawa estuary), X (the Arakawa and Old Edogawa estuaries), Y (off the coast of Area X), and Z (central part of Tokyo Bay). Throughout the monitoring, the $^{134+137}$Cs concentrations of surface sediments were highest in Area X and decreased significantly toward Area Z. The radioactivities of $^{134+137}$Cs are expressed as weighted averages; that in Area X is 424 Bq/kg (78–1340 Bq/kg, n = 55); Area Y, 131 Bq/kg (40–371 Bq/kg, n = 40); and Area Z, 17 Bq/kg (1–162 Bq/kg, n = 50). At the estuary of the Tamagawa River (Area V), which flows through the suburbs of western Tokyo, the weighted average is 57 Bq/kg (nd–234 Bq/kg, n = 8). At the estuary of the Sumidagawa River (Area W), which flows through central Tokyo, the weighted average is 103 Bq/kg (36–336 Bq/kg, n = 16). Both concentrations indicate lower contamination than in the Old Edogawa estuary (Area X). This distribution of radioactive cesium in Tokyo Bay sediments is in good agreement

with the pollution levels of radioactive cesium in the catchments of these incoming rivers.

From Fig. 6.2, radioactive cesium deposited in the sediments of Tokyo Bay is presumed to originate from the Old Edogawa and Edogawa rivers, which will are discussed in Sects. 6.7 and 6.8.

6.6.2 *Inventory and Flux of Radioactive Cesium in the Tokyo Bay Sediment*

The inventory and flux of radioactive cesium deposition in Tokyo Bay sediments from the basin based on the 5-year investigation of the FDNPP accident were estimated. Tables 6.2 and 6.3 show the inventory, flux, and $^{134}Cs/^{137}Cs$ activity ratio of radioactive cesium in sediments collected from Tokyo Bay and the Edogawa water system. The inventory was estimated for the samples in which the radioactive cesium contamination was confirmed to be due to the FDNPP accident by the vertical distribution of ^{134}Cs in the sediment core. The thickness of this contaminated sedimentary layer is also shown in the tables. The $^{134}Cs/^{137}Cs$ activity ratio of 117 sediment samples with a counting error of the activity readings within 5% is 1.006 ± 0.003 (weighted average), which is consistent with the radioactive cesium released by the FDNPP accident [30–32]. This agreement ensures the reliability of the measured data.

The inventory values of $^{134+137}Cs$ are 2.28–265 kBq/m^2 for Area X, 0.67–14.4 kBq/m^2 for Area Y, 0.04–6.10 kBq/m^2 for Area Z, 3.48–6.63 kBq/m^2 for Area W, and 0.00–11.0 kBq/m^2 for Area V. Area X in the Old Edogawa estuary shows an overwhelmingly large inventory compared to other marine areas of Tokyo Bay. This inventory reveals approximately the same pollution level as the radioactive cesium inventory of soils in highly contaminated areas in the middle of the Edogawa watershed. Additionally, since the concentration at Site A3 in the Arakawa River upstream of the Old Edogawa estuary decreases significantly, radioactive cesium that accumulated in Area X is assumed to have been supplied from the Old Edogawa and Edogawa water systems. Nevertheless, even if core samples were collected at the same sampling site, such as Site 02 or Site C, the inventory changed significantly on different sampling days. As described in Chap. 3, the soils contaminated by radioactive cesium show large local deviations. A similar trend is observed in the Tokyo Bay sediments. However, due to the physical mixing of seawater, it is unlikely that local segregation occurs during the process of radioactive cesium settling in the sea. Since the water depths at the sites where the cores were collected are as shallow as 5–10 m, radioactive cesium deposited on the sediment surface is probably disturbed by tidal currents. Nevertheless, the spatiotemporal distribution of radioactive cesium obtained at Site D suggests that the core at this point recorded a steady depositional process throughout the monitoring period. Therefore, the core

analysis taken from this site can be used for quantitative analysis of radioactive cesium contamination in Tokyo Bay.

Dividing the $^{134+137}$Cs inventory by the elapsed time (days) yields the average daily flux for sediment. The fluxes (arithmetic means) from the accident to the date of sediment collection are 0.084 ± 0.088 (n = 22) for Area X, 0.013 ± 0.010 (n = 13) for Area Y, 0.002 ± 0.003 (n = 50) for Area Z, 0.011 ± 0.010 (n = 6) for Area W, and 0.009 ± 0.014 (n = 8) kBq/m^2 day for Area V. The $^{134+137}$Cs flux in central Tokyo Bay is approximately 1/40 that in the Old Edogawa estuary. This large difference in flux in a narrow sea area such as Tokyo Bay suggests that radioactive cesium flowing into Tokyo Bay from the Old Edogawa was deposited in the estuary without diffusing into the bay. At Site D, where a steady depositional process is recorded, the average flux of the seven monitoring runs through July 2016 is 0.104 ± 0.019 kBq/m^2 day. The average flux for each collection period of the core sediments shown in Table 6.7 is 0.103 ± 0.051 kBq/m^2 day, which is evaluated as a typical representative value of the $^{134+137}$Cs flux in the Old Edogawa estuary due to the FDNPP accident.

6.6.3 *Spatiotemporal Fluctuations in Radioactive Cesium in the Tokyo Bay Sediment*

The vertical distributions of radioactive cesium in the sediments of Tokyo Bay and their temporal changes were investigated using core samples. Sediment cores were collected between August 2011 and July 2016 using a sampler with an inner diameter of 10 cm and a length of 100 cm. Figure 6.3 shows the vertical distribution of $^{134+137}$Cs radioactivity from the Old Edogawa estuary (Site 02) to the center of the bay (Site J) in 2014 and 2015. The highest activity of radioactive cesium was 1070 Bq/kg, which was detected in a layer at depths of 34–36 cm near the estuary, where the Old Edogawa flows. In this core, ^{134}Cs was detected until in the layer at depths of 54–56 cm. The concentration of radioactive cesium decreased rapidly in the layers shallower than 34–36 cm were $^{134+137}$Cs radioactivity peaked and measured 250–400 Bq/kg in the surface sediment layer. The vertical distribution of $^{134+137}$Cs in the Site 02 core has not been significantly affected by physical mixing despite its estuary location. This distribution suggests that contaminated suspended particles flowing from the Old Edogawa River steadily accumulated in this area. The vertical distribution of radioactive cesium showed a sharp decrease from the estuary (Site 02) to the inner part of Tokyo Bay (Site J). In the case of Site J, the peak $^{134+137}$Cs of 44 Bq/kg is detected in a 5 cm-deep layer. This distribution suggests that most of the radioactive cesium from the Old Edogawa was deposited rapidly in the estuary and scarcely diffused into the center of the bay. This behavior of radioactive cesium is fortunate in that the entire Tokyo Bay has not been exposed to massive radioactive contamination due to the FDNPP accident.

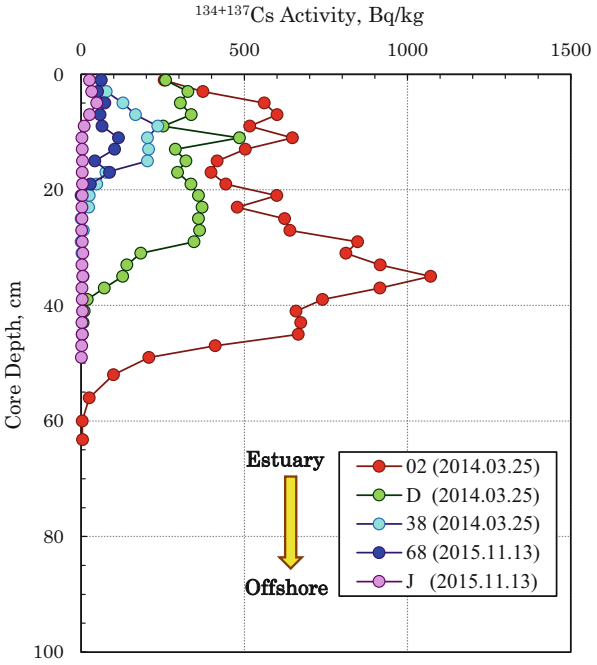

Fig. 6.3 Spatiotemporal changes in the vertical distribution of $^{134+137}$Cs in the sediment cores collected from the Old Edogawa estuary toward central Tokyo Bay. The date in the parentheses is the core collection date

Since core samples collected at Site D, 2.5 km south of the estuary of the Old Edogawa River, reveal the steadiest deposition, the temporal changes in the vertical distribution of radioactive cesium at this site are investigated. Site D is located 1.5 km south of Site 02 and is not significantly affected by the flow of river water from the Old Edogawa and Arakawa rivers. The results are shown in Fig. 6.4. In August 2011, in the sediment core that was quickly collected immediately after the FDNPP accident, the radioactive cesium concentration in the sediment was 284 Bq/kg in the 0–1 cm layer at the surface, but the highest level was 433 Bq/kg in the layer at depths of 4–6 cm. The peak in $^{134+137}$Cs moved to the layer at depths of 12–14 cm layer by October 2013, and its concentration was 547 Bq/kg. In July 2016, 5 years and 4 months after the accident, the peak of $^{134+137}$Cs was buried to a layer at depths of 64–66 cm. Although the peak concentration was 329 Bq/kg, the value corrected for radioactive decay since the time of the accident was 632 Bq/kg, indicating that the concentration peak of radioactive cesium more than 5 years after the accident had been buried but was retained in the sediment.

However, this peak depth does not necessarily indicate the history of the steady pollutant influx from the Old Edogawa River. Many rivers flooded in the Tokyo metropolitan area due to the Kanto-Tohoku heavy rain from September 9–11, 2015. As discussed in Sect. 6.6, the Edogawa water system also flooded. The flood carried material down the river and into Tokyo Bay. As shown in Fig. 6.5, traces of flood sediments were recorded as anomalies in water content and porosity (deposits of low-density sediments) in the layers at depths of 8–22 cm collected in November

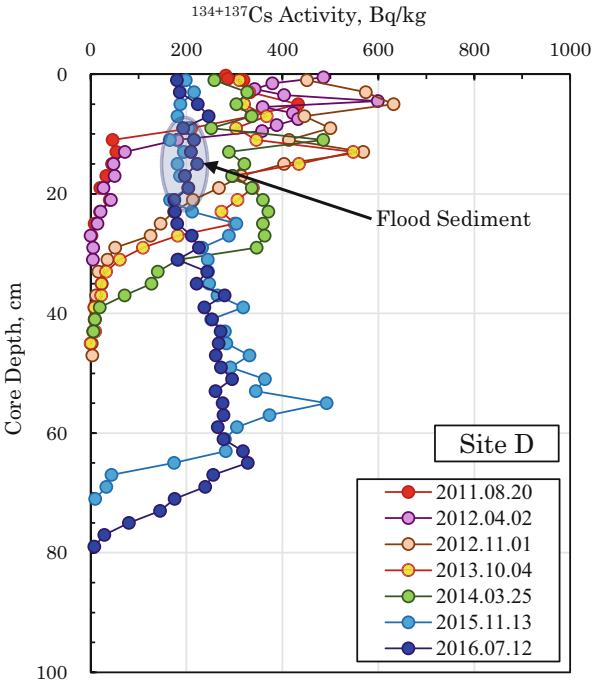

Fig. 6.4 Temporal changes in the vertical distribution of $^{134+137}$Cs in the sediment core collected at Site D. The black circle in the core collected on Nov. 13, 2015, shows the flood sedimentary layer that flowed in due to the Kanto-Tohoku heavy rainfall from September 9–11, 2015

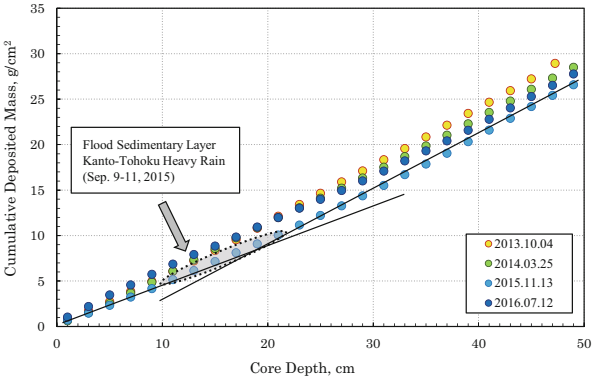

Fig. 6.5 Evidence for the flood sediment deposited at Site D. Coastal flood sediments have high water content and small particle size, so their apparent density will be smaller [33]. The cumulative mass of 8–22 cm layer in the core collected on November 13, 2015, is lower than that of the other cores

2015. It is known that sediments with high water content and low apparent density accumulate in estuaries during floods [33]. In other words, the cores collected in November 2015 and July 2016, shown in Fig. 6.4, had flood sediment layers with thicknesses of 10 cm or more. A quantitative analysis of the distribution of radioactive cesium in the Site D core is discussed in Sect. 6.8.

6.7 Spatiotemporal Distributions of Radioactive Cesium in the Sediments of the Old Edogawa, Edogawa, and Sakagawa Rivers

6.7.1 Concentration of Radioactive Cesium in the Sediment of the Edogawa Water System

As Sects. 6.5 and 6.6 clearly indicate, the source of radioactive contamination in Tokyo Bay is presumed to be the Edogawa River system. The downstream reach of the Edogawa River from Gyotoku Weir has been renamed the Old Edogawa River, as shown in Fig. 6.2. This weir is closed except during a major flood, when the water of the Edogawa River flows into the Old Edogawa River. Most of the river water flows into Tokyo Bay near Site 33 in Fig. 6.1, but some water also flows near Site 03. The middle watershed of the Edogawa River is a highly contaminated area due to the FDNPP accident. This contaminated area is the catchment area of the Sakagawa River, which joins the Edogawa River. Table 6.4 shows the concentrations of radioactive cesium in the soils of the Sakagawa River catchment area collected in 2011 and those of the Sakagawa riverbank collected in 2014. The radioactive cesium concentrations are higher in the catchment area than in the riverbank.

Table 6.3 shows the radioactive decay-corrected $^{134+137}$Cs concentrations of surface sediments at depths of 0–5 cm in the Edogawa and Nakagawa rivers. The weighted average $^{134+137}$Cs concentration in the Sakagawa surface sediment is 1760 ± 8 Bq/kg (n = 8, 0–5 cm). This concentration indicates that the soil contaminated with radioactive cesium is transported from the catchment areas, and deposited in the Sakagawa sediment. The Edogawa River branches off from the Tonegawa River, but according to the results of airborne monitoring [1] in Fig. 3.2, the forested area in Gunma Prefecture upstream of the Tonegawa River is contaminated with 60–300 kBq/m^2 of radioactive cesium. However, upstream of the Edogawa River branching off from the Tonegawa River, the concentration of $^{134+137}$Cs in the sediment is 170 ± 2 Bq/kg (n = 20, Sites E1–E4), and that at the downstream sites in the Sakagawa River is 473 ± 3 Bq/kg (n = 14, Sites E5–E10). Therefore, the contaminated area upstream of the Tonegawa River is not considered an essential source of radioactive cesium to supply Tokyo Bay. On the other hand, radioactive cesium deposited in the Sakagawa catchment in the northern part of Chiba Prefecture is estimated to be a significant source of pollution in Tokyo Bay.

6.7.2 Inventories and Fluxes of Radioactive Cesium in the Sediments of the Edogawa and Sakagawa Rivers

The Matsudo Weir is located about 30 m downstream from Site S1 and is usually closed to regulate the water flow in the Sakagawa River. Therefore, the flow velocity

Table 6.4 Concentrations and inventories of radioactive cesium in soil samples collected around Sakagawa River

Site	Sampling date	Detected, Bq/kg			Corrected[a], Bq/kg			Inventory, kBq/m^2	^{134}Cs/^{137}Cs ratio
		^{134}Cs	^{137}Cs	$^{134+137}$Cs	^{134}Cs	^{137}Cs	$^{134+137}$Cs		
K1	2011/5/19	3010 ± 22	3170 ± 24	6180 ± 33	3210 ± 24	3180 ± 24	6390 ± 34	83	1.009 ± 0.011
K2	2011/6/11	31,200 ± 97	33,700 ± 101	64,900 ± 140	33,900 ± 105	33,900 ± 102	67,800 ± 146	881	1.000 ± 0.004
K3	2011/6/11	16,300 ± 60	17,600 ± 66	33,900 ± 89	17,700 ± 65	17,700 ± 66	35,400 ± 93	460	1.000 ± 0.005
K4	2011/5/19	970 ± 12	1070 ± 13	2040 ± 18	1060 ± 13	1080 ± 13	2140 ± 18	57	0.982 ± 0.017
S5	2014/4/29	168 ± 4	452 ± 7	620 ± 8	480 ± 13	485 ± 7	965 ± 15	25	0.990 ± 0.030
S4	2014/4/29	904 ± 22	2480 ± 34	3380 ± 41	2580 ± 62	2660 ± 37	5250 ± 72	137	0.970 ± 0.027
S6	2014/4/29	445 ± 12	1140 ± 18	1590 ± 22	1270 ± 33	1230 ± 20	2500 ± 39	65	1.033 ± 0.032
S3	2014/4/29	391 ± 10	1020 ± 16	1410 ± 19	1120 ± 29	1100 ± 17	2220 ± 34	58	1.018 ± 0.031
S2	2014/4/29	271 ± 6	700 ± 10	971 ± 12	775 ± 18	752 ± 11	1530 ± 21	40	1.031 ± 0.028
S1	2014/4/29	551 ± 15	1480 ± 23	2030 ± 28	1580 ± 42	1590 ± 25	3170 ± 49	82	0.994 ± 0.031

The K series samples are the soil of the residential areas, and the S series samples are the soil of the Sakagawa riverbank

[a]Decay-corrected value to March 16, 2011

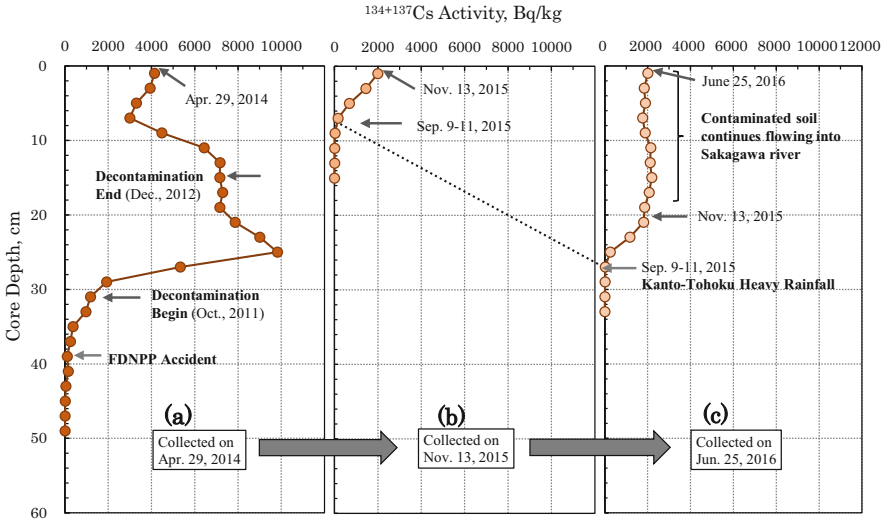

Fig. 6.6 (**a**–**c**) Temporal changes in the vertical distribution of $^{134+137}$Cs in the sediment core at Site S1 in Sakagawa River. When the Matsudo weir was opened because of the Kanto-Tohoku heavy rainfall, large proportions of the contaminated sediment deposited at Site S1 flowed out. Decontamination works in Kashiwa City were carried out between "Begin" and "End" in figure (**a**) [34]

of water in the Sakagawa River decreases rapidly above this weir, meaning that suspended solids are deposited at this point. Table 6.3 shows the radioactive cesium concentrations in the surface sediments (0–5 cm depths) of the Sakagawa and Edogawa rivers from upstream to downstream. In the Edogawa River, the radioactive cesium concentration increases approximately 2.8 times from Sites E1–E4 upstream of the confluence with the Sakagawa River to Sites E5–E10 downstream. Since the Sakagawa is a narrow river with a complicated flow path, the concentrations of radioactive cesium fluctuate greatly depending on the sediment sampling point. Nevertheless, the concentration of radioactive cesium in Sakagawa sediments is approximately 10–40 times higher than that in the upper Edogawa. These values indicate that the contamination of Edogawa sediment by radioactive cesium supplied from the Sakagawa River. The soil in the catchment area of the Sakagawa is highly radioactively contaminated and provides a credible origin for the radioactive cesium in the region. The results suggest that the behavior of radioactive cesium in this water system can be estimated from its inventory and flux.

Figure 6.6 shows the vertical distribution of radioactive cesium in the sediment core at Site S1. The vertical distribution of radioactive cesium before and after the FDNPP accident was recorded in the S1(a) core sampled on April 29, 2014. If it is presumed that the 38–40 cm layer in which ^{134}Cs is detected was deposited immediately after the accident, the rate of deposition of this sediment is approximately 1.0 cm/month. Thus, as shown in Fig. 6.6a, the sediment layer deposited in October 2011 is the layer from 32 to 34 cm; this time is when decontamination work started in Kashiwa City [34], which is in the catchment area of the Sakagawa River. The

decontamination work was completed in December 2012, and the sedimentary layer corresponds to a depth of 14–16 cm. For this reason, as shown in Fig. 6.6a, the vertical distribution of $^{134+137}$Cs in core S1(a) records the radioactive sludge discharge history due to decontamination work in Kashiwa City. Presumably, the radioactive cesium in the highly contaminated layer represents contaminated soil from the high-contamination zone accompanied by a discharge of contaminated sludge caused by the decontamination work in Kashiwa City. Some of the decontamination wastewater that was not properly treated flowed into the Sakagawa River, and it is highly likely that this contaminated sludge was deposited at Site S1.

However, eastern Japan, including the Tokyo metropolitan area, experienced heavy rain called the Kanto-Tohoku heavy rainfall between September 9 and 11, 2015. The total precipitation in the watershed of the Tokyo metropolitan area was more than 500 mm, and many rivers flooded. More than 200 mm of rain also fell on the Sakagawa catchment area [35–37]. A new sediment core S1(b) was collected at the same location as the S1(a) core on November 13, 2015, approximately 3 months after the heavy rain event. Figure 6.6b shows the analytical results for this core. The highly contaminated sediment layer observed in core S1 (a) disappeared, but new contaminated sediment was deposited after the flood. A newer core S1(c) was also collected on June 25, 2016, approximately 10 months after the flood event. The mass fluxes of these sediment cores are shown in Table 6.5. The mass flux of core S1(b) is considerable, indicating that the sedimentation process at this point was strongly affected by flooding. Throughout the entire sedimentation period, the concentrations of $^{134+137}$Cs in the sediment are 3000–10,000 Bq/kg for S1(a) and approximately 2000 Bq/kg for S1(b) and S1(c). After the flood event, no highly contaminated sediment flowed in, but approximately 2000 Bq/kg of contaminants continued to flow into the Sakagawa River. Perhaps a large influx of low-contamination soil could also have diluted the radioactive cesium concentration. The temporal changes in inventory and flux at Site S1 site were calculated using these measurement results. The results are shown in Table 6.5.

From the mass fluxes and radioactive cesium concentrations shown in Table 6.5, the inventory and flux for each sampling period can be calculated. The $^{134+137}$Cs fluxes of the S1(a), (b), and (c) cores were 0.997 kBq/m^2 day, 1.03 kBq/m^2 day, and 0.993 kBq/m^2 day, respectively, after decay correction to the values on March 16, 2011. From immediately after the FDNPP accident until June 2016, the radioactive cesium flux at the Sakagawa Site S1 did not change at all. Furthermore, as shown in parentheses in Table 6.5, this flux decreased with the radioactive decay of $^{134+137}$Cs (Fig. 6.7). The value was 0.517 kBq/m^2 day in June 2016. These values suggest that the amount of radioactive pollutants flowing into the Sakagawa River from its catchment areas remained constant for 5 years after the accident. The $^{134+137}$Cs flux at Site D offshore from the Old Edogawa estuary, which is downstream of the Sakagawa and Edogawa rivers, is approximately 0.05 kBq/m^2 day (Fig. 6.8), so the $^{134+137}$Cs flux of Site S1 is approximately ten times higher than that at Site D.

In any case, the amount of radioactive cesium supplied from the contaminated land to Tokyo Bay, excluding the effects of decreases due to radioactive decay, changed little during the 5 years after the FDNPP accident. A more detailed analysis of where this radioactive cesium on land originated is required.

Table 6.5 Concentrations, inventories, and fluxes of radioactive cesium in the sediment at Site S1 in Sakagawa River

Sampling date	Core depth, cm	Sampling interval	Elapsed time[a], day	Total mass, kg/m^2	Mass flux, kg/m^2 day	Activity[b], kBq/kg			Inventory[b], kBq/m^2			Flux[b], kBq/m^2 day
						^{134}Cs	^{137}Cs	^{134}+^{137}Cs	^{134}Cs	^{137}Cs	^{134}+^{137}Cs	$^{134+137}$Cs
2014/4/29 Figure 6.6a	0–44	2011/3/16 2014/4/29	1140 (1140)	163	0.143	3.50 (1.22)	3.46 (3.22)	6.96 (4.45)	571 (200)	565 (526)	1140 (726)	0.997 (0.637)
2015/11/13 Figure 6.6b	0–10[c]	2015/9/11[d] 2015/11/13	63 (1703)	50.5	0.802	0.66 (0.14)	0.65 (0.58)	1.30 (0.72)	33 (7)	33 (29)	66 (36)	1.030 (0.575)
2016/6/25 Figure 6.6c	0–26	2015/9/11[d] 2016/6/25	288 (1928)	89.0	0.309	1.62 (0.28)	1.58 (1.40)	3.20 (1.67)	145 (24)	141 (124)	285 (149)	0.993 (0.517)
	20–26[c]	2015/9/11[d] 2015/11/13	63 (1928)	30.7	0.487	1.01 (0.17)	1.03 (0.92)	2.05 (1.09)	31 (5)	32 (28)	63 (33)	0.996 (0.529)
	0–20	2015/11/13 2016/6/25	225 (1928)	58.3	0.259	1.94 (0.33)	1.87 (1.65)	3.81 (1.98)	113 (19)	109 (96)	222 (116)	0.987 (0.513)

[a]The value in parentheses is days from March 16, 2011
[b]Decay-corrected value to March 16, 2011. The value in parentheses is detected value for the interval examined
[c]These sedimentary layers deposited at the same time
[d]The contaminated sediment layer was flowed out due to the Kanto-Tohoku heavy rainfall on September 9–11, 2015

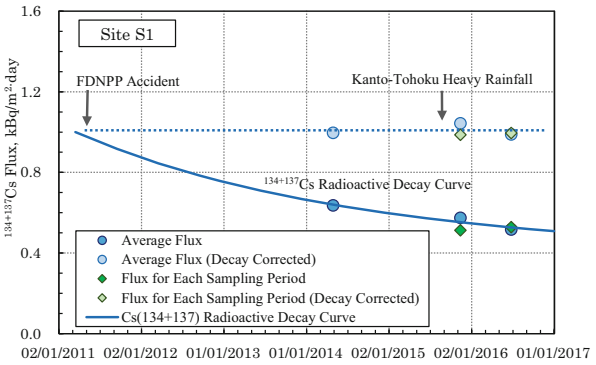

Fig. 6.7 Temporal changes in fluxes of $^{134+137}$Cs to the sediment at Site S1 in Sakagawa River

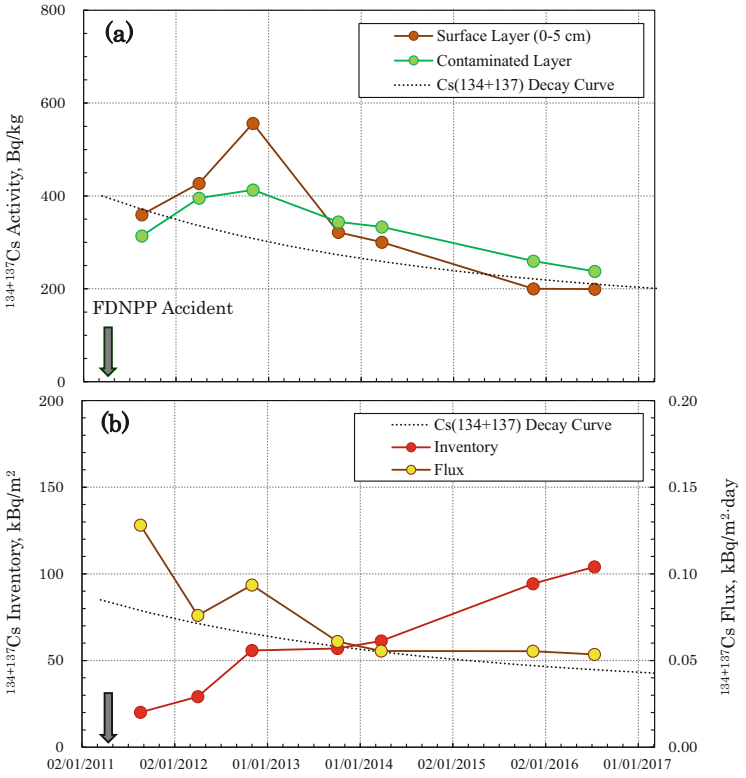

Fig. 6.8 (**a**, **b**) Temporal changes in concentrations, inventories, and fluxes of $^{134+137}$Cs at Site D in the estuary sediment of Old Edogawa River. The contaminated layer was defined as the layer including the detectable ^{134}Cs. Flux was calculated by dividing the inventory by elapsed time since the FDNPP accident

6.8 Source, Migration, and Deposition of Radioactive Cesium in the Tokyo Bay Water System

6.8.1 Inventory and Flux of Radioactive Cesium Due to the FDNPP Accident in the Sediment at Site D in the Old Edogawa Estuary

As shown in Fig. 6.2 and Table 6.3, the radioactive cesium concentrations in sediments in the Edogawa River system increase in the order of Sakagawa-lower Edogawa-upper Edogawa. This order suggests that radioactively contaminated soil that has flowed into the Sakagawa from highly contaminated areas around Kashiwa and Matsudo cities is transported to Tokyo Bay via the Edogawa and Old Edogawa rivers. In other words, the source of radioactive cesium contamination in Tokyo Bay is contaminated soil in highly polluted areas, and the Edogawa River system is considered to play an essential role in its transport. Based on the vertical distribution of radioactive cesium in the core sediment deposits at Site D, as shown in Fig. 6.4, the changes over time in the activity, inventory, and flux of the $^{134+137}$Cs in the sediment were analyzed.

Table 6.6 shows the temporal changes in the concentration of radioactive cesium in the sediments and inventory at Site D, offshore from the estuary where the Old Edogawa River flows into Tokyo Bay. The $^{134+137}$Cs concentrations of the surface 0–5 cm layer and the total radioactively contaminated layers were the highest in the sediment collected in November 2012. As shown in Table 6.7, the daily flux of $^{134+137}$Cs for each sampling period also peaked in November 2012 when the concentration maximum. These values mean that it took approximately one and a half years for the contaminated soil in the Sakagawa catchment area to be transported to Tokyo Bay. The inventory of $^{134+137}$Cs increased from 20 to 104 kBq/m^2 during the 4 years and 11 months from August 2011 to July 2016. Theoretically, by July 2016, the $^{134+137}$Cs activity should have decayed to 53% of the value immediately after the accident. The inventory increased by five times despite the ^{134}Cs decrease due to radioactive decay. This increase suggests that even now, radioactive cesium continues to flow into Tokyo Bay constantly. Table 6.7 shows the average flux of $^{134+137}$Cs at Site D and the flux for each sampling period calculated from the values in Table 6.6. The estimated average flux immediately after the accident was 0.128 kBq/m^2 day, but by July 2016, it had decreased to 0.054 kBq/m^2 day. The flux estimated for each sampling period fluctuates significantly from 0.003 to 0.128 kBq/m^2 year (0.059–0.177 kBq/m^2 day after decay correction).

However, both average fluxes are approximately 0.103–0.104 kBq/m^2 day after 5 years and 4 months had passed since the FDNPP accident, but the material that flows and accumulates in Tokyo Bay has not changed much over time. This flux is approximately 10% of that at Sakagawa Site S1, which is the contamination source. These results are shown in Fig. 6.8. The radioactive decay curve of the $^{134+137}$Cs activity is based on the hypothesis that the ^{134}Cs/^{137}Cs activity ratio emitted during the accident was 1.0 [30–32]. In the post-2013 period, when the dynamics of

Table 6.6 Concentrations and inventories of radioactive cesium in the sediments collected at Site D in the Old Edogawa estuary

Sampling date	Elapsed time[a], day	$^{134+137}$Cs activity, Bq/kg					Inventory[c], kBq/m^2						Ratio ^{134}Cs/^{137}Cs[d]
		Surface layer, 0–5 cm		Contaminated Layer[b]			^{134}Cs		^{137}Cs		$^{134+137}$Cs		
		Detected	Corrected	Depth, cm	Detected	Corrected	Detected	Corrected	Detected	Corrected	Detected	Corrected	
2011/8/20	157	360	388	0–26	314	338	9.3	10.7	10.8	10.9	20.1	21.7	0.991 ± 0.021
2012/4/2	383	427	509	0–26	395	471	12.1	17.2	17.0	17.4	29.4	35.0	0.989 ± 0.009
2012/11/1	596	556	721	0–44	413	538	21.1	36.5	34.7	36.0	55.8	72.6	1.014 ± 0.015
2013/10/4	933	322	471	0–44	344	512	17.7	41.9	39.2	41.6	56.9	83.4	1.007 ± 0.012
2014/3/25	1105	300	465	0–42	334	518	17.2	47.7	44.1	47.3	61.5	95.1	1.008 ± 0.013
2015/11/13	1703	200	366	0–70[e]	260	473	18.0	86.4	76.3	84.9	94.3	171	1.018 ± 0.012
2016/7/12	1945	200	379	0–78[e]	238	456	16.9	101	87.1	98.5	104	200	1.025 ± 0.015
											Weighted average[d]		1.007 ± 0.005

Detected: Value on the sampling date. Corrected: Decay-corrected value to March 16, 2011

[a]Days from March 16, 2011

[b]Contaminated layer is the thickness from the surface to the deepest layer where ^{134}Cs is detected

[c]Cumulative value from March 16, 2011, to the sample collection

[d]Weighted average value in each layer of the core

[e]Sedimentary layer included the layer of 14 cm thickness deposited by the flood from August 9–11, 2015

Table 6.7 Fluxes of radioactive cesium in the sediments collected at Site D in the Old Edogawa estuary

Sampling date	Elapsed time, day	Sampling interval, day	Average flux[a], kBq/m^2 day						Each sampling interval			
			^{134}Cs		^{137}Cs		$^{134+137}$Cs		Inventory, kBq/m^2		Flux, kBq/m^2 day	
									$^{134+137}$Cs		$^{134+137}$Cs	
			Detected	Corrected	Detected	Corrected	Detected	Corrected	Detected	Corrected	Detected	Corrected
2011/8/20	157	157	0.059	0.068	0.069	0.070	0.128	0.138	20.1	21.7	0.128	0.138
2012/4/2	383	226	0.032	0.045	0.044	0.046	0.076	0.091	9.3	13.3	0.041	0.059
2012/11/1	596	213	0.035	0.061	0.058	0.060	0.094	0.122	26.4	37.6	0.124	0.177
2013/10/4	933	337	0.019	0.045	0.042	0.045	0.061	0.089	1.1	10.8	0.003	0.032
2014/3/25	1105	172	0.016	0.043	0.040	0.043	0.056	0.086	4.6	11.7	0.027	0.068
2015/11/13	1703	598	0.011	0.051	0.045	0.050	0.055	0.100	32.8	75.9	0.055	0.127
2016/7/12	1945	242	0.009	0.052	0.045	0.051	0.054	0.103	9.7	29.0	0.040	0.120
						Average		0.104 ± 0.019	Average			0.103 ± 0.051

Detected: Value on the sampling date. Corrected: Decay-corrected value to March 16, 2011

[a]Average value from March 16, 2011, to the date of sample collection

contamination seem to have reached a steady state, the fluctuations in radioactive cesium concentration and inventory in Site D sediments are almost consistent with the decrease due to radioactive decay of $^{134+137}$Cs. This fact means that the constant inflow of ^{137}Cs with a long half-life into Tokyo Bay continues even after ^{134}Cs has disappeared. The annual supply of radioactive cesium in Area X is assumed to be approximately 0.24 TBq (see Sect. 6.9).

6.8.2 *Contamination via Global Fallout of ^{137}Cs in Tokyo Bay Sediment Before the FDNPP Accident*

Information on the radioactive cesium concentration in Tokyo Bay sediment before the FDNPP accident was relatively deficient compared to that for Japanese water samples [38]. However, clarifying the background concentration and flux of radioactive cesium flowing into Tokyo Bay is very important for evaluating radioactive cesium contamination in Tokyo Bay caused by the FDNPP accident. The global fallout from atmospheric nuclear tests started in the 1950s and was an essential source of ^{137}Cs pollution in the environment before the Chernobyl and FDNPP accidents. In Japan, global fallout measurements began in 1954. Figure 6.9 shows the annual precipitation measured by NIRS in Chiba City on the east coast of Tokyo Bay [39]. The global fallout reached its maximum value of 1.585 kBq/m^2 in 1963 but has since decreased sharply and was less than 0.001 kBq/m^2 in 1984. However, it increased to 0.161 kBq/m^2 in 1986 when the Chernobyl nuclear accident occurred and decreased to 0.002 kBq/m^2 in 1987. In other words, the background level of

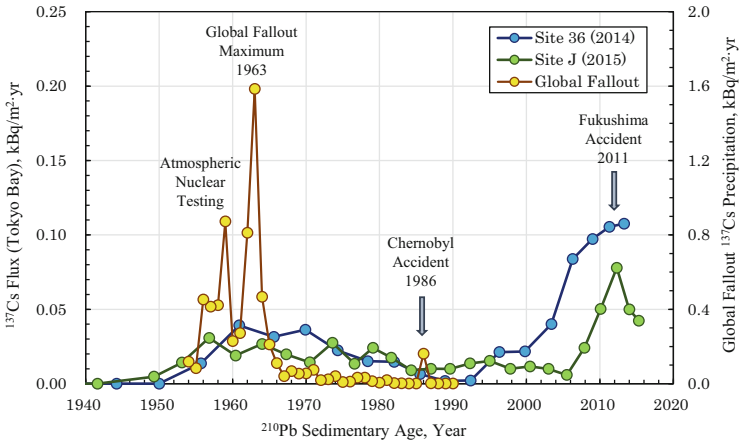

Fig. 6.9 Nuclear events prior to the FDNPP accident recorded in the sediment cores in central Tokyo Bay. Annual precipitations of ^{137}Cs by atmospheric global fallout were measured by NIRS in Chiba City in the east of Tokyo Bay [39]

^{137}Cs in Tokyo Bay is less than 0.001 kBq/m^2 at present, and it is not necessary to consider the effects of the Chernobyl accident.

The inventory of ^{137}Cs in the Tokyo Bay sediment has already been reported as 0.37–0.51 kBq/m^2, but this value might be underestimated due to the short core used in the analysis [38]. The cores from Site 36 (taken in 2014) and Site J (taken in 2015) shown in Fig. 6.9 were dated using the ^{210}Pb method. The deepest layers where ^{137}Cs was detected were 32–34 cm (1956) at Site 36 and 48–50 cm (1948) at Site J. The ^{134}Cs derived from the FDNPP accident was found in upper layers of 8–10 cm (2003) at Site 36 and 12–14 cm (2003) at Site J. This distribution of ^{134}Cs is reasonable, given the effect of physical mixing of the sediments. However, the sedimentation rate increased at Site J, which is far from the mouths of the Arakawa and Old Edogawa rivers. The average concentrations of ^{137}Cs in these cores from 1955 to 1970, when global fallout was remarkable, are 16.8 ± 6.8 Bq/kg for Site 36 and 10.6 ± 3.1 Bq/kg for Site J. These results may indicate that Site J is affected by the dilution effect of suspended particle flow from the Tamagawa and Tsurumigawa rivers.

In addition, in the 1954–1985 sedimentary deposits before the Chernobyl accident, the inventories of ^{137}Cs are 0.796 kBq/m^2 at Site 36 and 0.713 kBq/m^2 at Site J. These inventories are slightly larger than previously reported [38]. Since the global fallout inventory at this time was 6.56 kBq/m^2, the ^{137}Cs inventory in central Tokyo Bay is approximately 11–12% of the global fallout. However, between 1954 and 1985, the ^{137}Cs global fallout must have been precipitated onto the surface of the seawater, so the inventories recorded in the sediment cores are quite small. Presumably, ^{137}Cs, which moved directly from the atmosphere into seawater due to global fallout, was likely to have been dissolved in seawater and not deposited on the seafloor.

On the other hand, the average fluxes of ^{137}Cs in Tokyo Bay sediment resulting from atmospheric nuclear tests were 0.027 kBq/m^2 year at Site 36 and 0.024 kBq/m^2 year at Site J. As shown in Fig. 6.8, the flux of $^{134+137}$Cs at Site D offshore of the Old Edogawa estuary was approximately 19.7 kBq/m^2 year (0.054 kBq/m^2 day) in 2016. In other words, radioactive cesium due to the FDNPP accident continues to flow into Tokyo Bay at a rate that is more than 700 times faster than that in the era of atmospheric nuclear tests.

6.8.3 Estimation of the Sedimentation Process for Radioactive Cesium in the Edogawa Water System and Tokyo Bay

A model calculation was conducted, and the movement process of radioactive cesium from the land to the aquatic system was simulated based on values observed in various environments [40–43]. The results in Figs. 6.2 and 6.3 show that radioactive cesium deposited on the ground surface in the northeastern part of the Tokyo metropolitan accumulated in the estuaries in the inner part of Tokyo Bay but did not

diffuse to the center of the bay. The fact that radioactive cesium was selectively deposited in the estuaries suggests that radioactive cesium adsorbed onto suspended particles large enough to settle quickly when they enter Tokyo Bay. Therefore, the particle size distribution of sedimentary materials was measured in the Tokyo Bay and Edogawa water systems. Figure 6.10 shows the analytical results for the particle size distribution calculated on a volume basis.

The average particle size of the park soil in Kashiwa City, which is a highly contaminated area, is approximately 80 μm but is divided into three sizes: 5–10, 20–80, and 200–800 μm at Site S5 in the Sakagawa headwaters. The large particles are not washed away by the river water but are likely to remain in place. Site S1 is the point where the Sakagawa merges with the Edogawa. Since the Matsudo Weir blocks the flow, the flow velocity of the water decreases. The average particle size of the sediment is approximately 10 μm, as fine particles less than 0.5 μm in size are also deposited (red circle in Fig. 6.10). The average grain size of sediments decreases from the Old Edogawa estuary to offshore. Site 02 has 30% of 50–200 μm particles and Site D has approximately 10% of 50–100 μm particles. At Site 52, approximately 6 km offshore from Site D, these large particles disappear, and the fraction of particles with sizes of 10 μm or smaller increases. These results mean that the contaminated particles flowing from the Old Edogawa River are spreading in this estuary area, with the large particles settling there first. This size distribution suggests that the coagulated deposition of colloidal particles by salting out did not occur in the estuary. Because the average particle size of the sediment decreases from the estuary toward the offshore area, large particles among sedimentary substances flowing from the river accumulate first as they diffuse through the seawater. If Stokes' law is applied in a simplified manner, the settling velocity of suspended particles would be 0.07 m/day at 1 μm, 1.7 m/day at 5 μm, 7 m/day at 10 μm, and 170 m/day at 50 μm. These results suggest that radioactive cesium deposited in the Old Edogawa estuary had adsorbed onto relatively large particles with particle sizes of approximately 5–50 μm.

Cesium cations are well known to penetrate between layers of 2:1 clay minerals, such as vermiculite and mica, and are strongly immobilized by ionic adsorption [44–49]. Thus, radioactive cesium precipitated on the surface from the atmosphere is retained by adsorbing onto clay minerals in the soil. Recently, it was directly confirmed that radioactive cesium released from the FDNPP was adsorbed onto clay minerals using new technologies such as EXAFS and NMR [50–52]. In addition, fine particles of radioactive cesium with high specific activity, so-called cesium balls or hot particles, have been found in eastern Japan [53–57]. However, when radioactive cesium is present in the air in gaseous form or as ultrafine dust, the effect of a washout due to rainfall is thought to play an essential role in the deposition of radioactive cesium on the ground. Although the physicochemical species of mobile radioactive cesium observed in the early days of the FDNPP accident are not precise, the presence of fine particles from radioactive cesium solid solutions such as cesium balls can also be noted. However, in Tokyo Bay, radioactive cesium deposited on the ground surface can be considered to have been adsorbed onto fine clay minerals in the soil and transported to the estuaries around Tokyo Bay. In this case, it is assumed

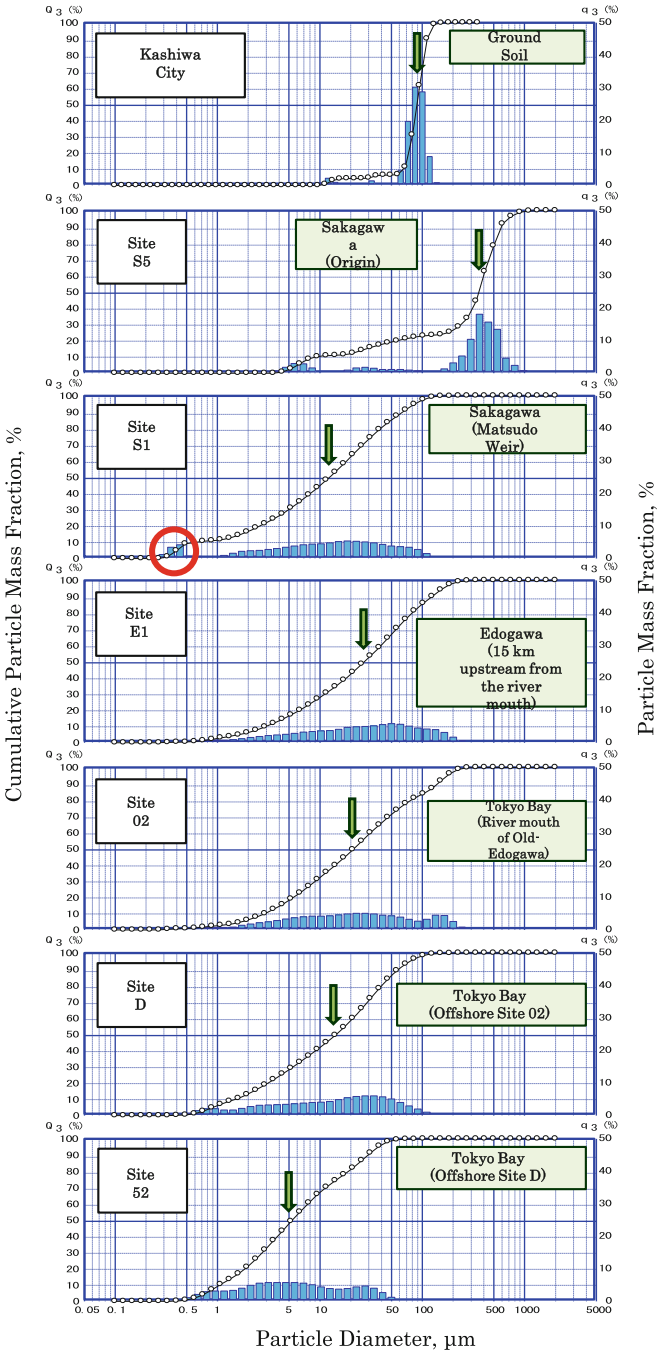

Fig. 6.10 Geographic changes in the particle size distributions of surface sediments in the Tokyo Bay water system. The vertical arrow indicates the average particle diameter

that when river water mixes with seawater, the contaminated fine particles settle to the seabed due to the salting-out effect associated with seawater [44, 58, 59]. Moreover, the coagulum accumulates in estuary sediments. However, such a depositional mechanism cannot explain the distribution of radioactive cesium in Tokyo Bay. Anthropogenic heavy metal elements also flow into Tokyo Bay through a process similar to that for radioactive cesium. Therefore, the distributions of radioactive cesium and heavy metals in Tokyo Bay were compared.

Anthropogenic heavy metal concentrations in the surface sediments of Tokyo Bay were estimated, assuming that concentrations in the age before the Meiji Restoration (1868), when industrial modernization began in Japan, were the natural background values. The background concentrations were 100 mg/kg for zinc, 40 μg/kg for mercury, and 10 mg/kg for lead. As shown in Fig. 6.11, an apparent particle size effect between the concentration of heavy metals and the average sediment particle size in the Tokyo Bay water system was confirmed. If the sedimentary particles are assumed to be spherical, the concentrations of radioactive cesium and heavy metals in the sediment must follow the inverse square law for the size of the sedimentary particles [58–60]. This figure illustrates that heavy metals selectively accumulate in the sediments in central Tokyo Bay, where the average particle size of the heavy metals is relatively small. This phenomenon occurs when heavy metals artificially flow into the aquatic environment and are adsorbed onto the surfaces of suspended particles in water. Nevertheless, the slope is less than 2. Since many rivers flow into Tokyo Bay, there may be a dilution effect due to suspended fine particles with low anthropogenic heavy metal contamination. Additionally, larger particle sizes deviate slightly from the inverse square law. This bias is probably due to the relatively high background concentration of sediment components, as the effect of heavy metal leaching during the advection process is smaller for larger particles.

As shown in Fig. 6.12, unlike the case of heavy metals, no negative correlation is found between radioactive cesium concentration and particle size. The average particle size of the soil in the highly contaminated zone is generally 50–100 μm, and the radioactive cesium activity ranges from 1000 to 35,000 Bq/kg. The source of radioactive cesium contamination in Tokyo Bay is believed to be flows from the highly contaminated areas of the Sakagawa catchment area. When flowing into the Sakagawa, sediments are classified into average particle sizes of 8–20 μm (4000–35,000 Bq/kg) and 250–350 μm (1500–6000 Bq/kg). Large particles settle in the Sakagawa River, and small particles move to the junction with the Edogawa River. From the Sakagawa River to Tokyo Bay, there appears to be a positive correlation between particle size and radioactive cesium concentration, in contrast to the particle size effects observed for heavy metals. This distribution suggests that radioactive cesium is not adsorbed onto suspended particles in the water during transport from the Sakagawa River to Tokyo Bay. In other words, the polluted particles deposited in Area X of Tokyo Bay are soil particles with a particle size of several micrometer to several tens of micrometer that have adsorbed large amounts of radioactive cesium in the Sakagawa catchment area. The low radioactivity of radioactive cesium in Area Z in central Tokyo Bay, where the sediment particles are small, is thought to be due to the dilution effect of particles with low contamination

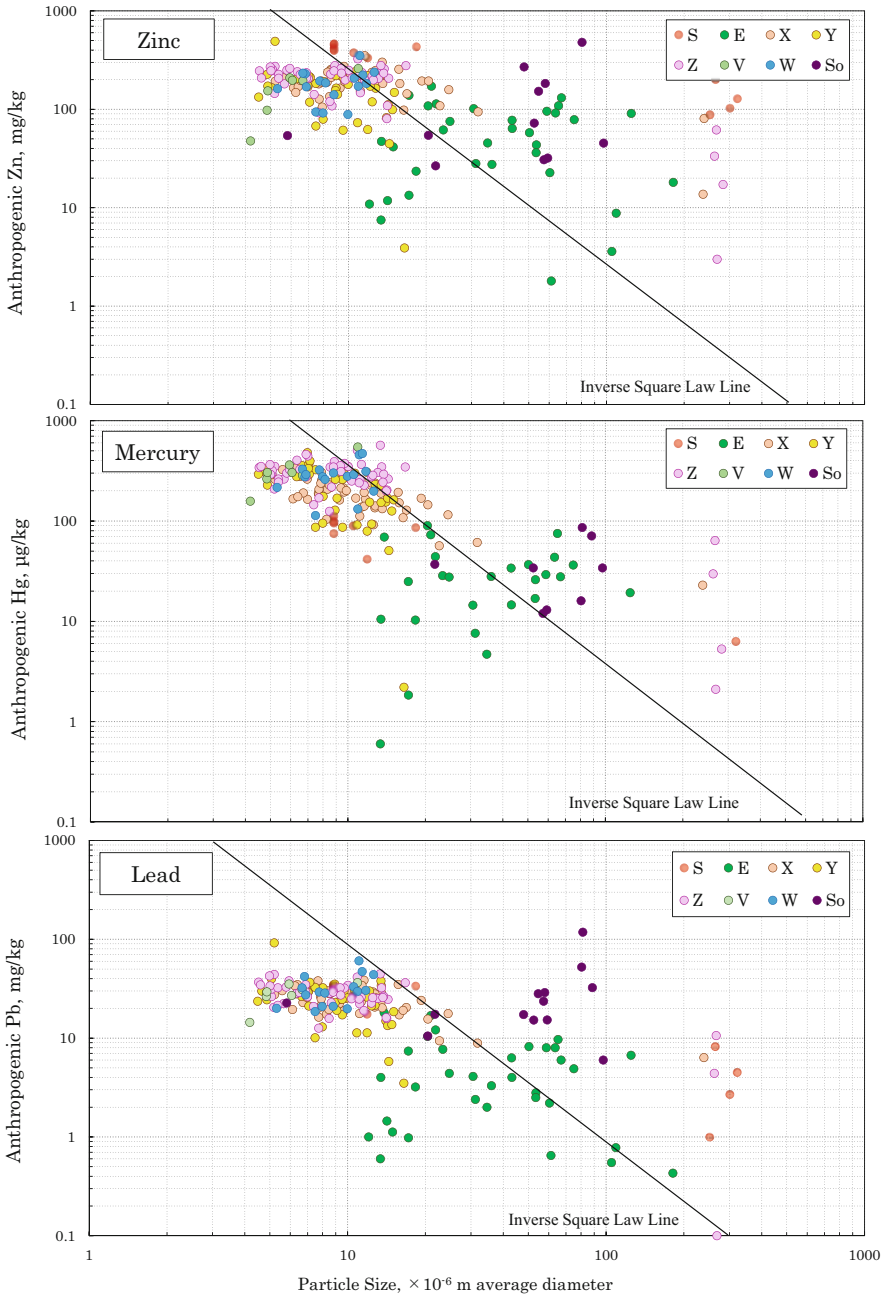

Fig. 6.11 Relationship between the anthropogenic heavy metal concentrations and the particle size of surface sediments in the Tokyo Bay water system. The anthropogenic concentrations of heavy metals were estimated assuming that the concentrations of sediments collected in Tokyo Bay deposited older than 1900 are the background concentration [2]

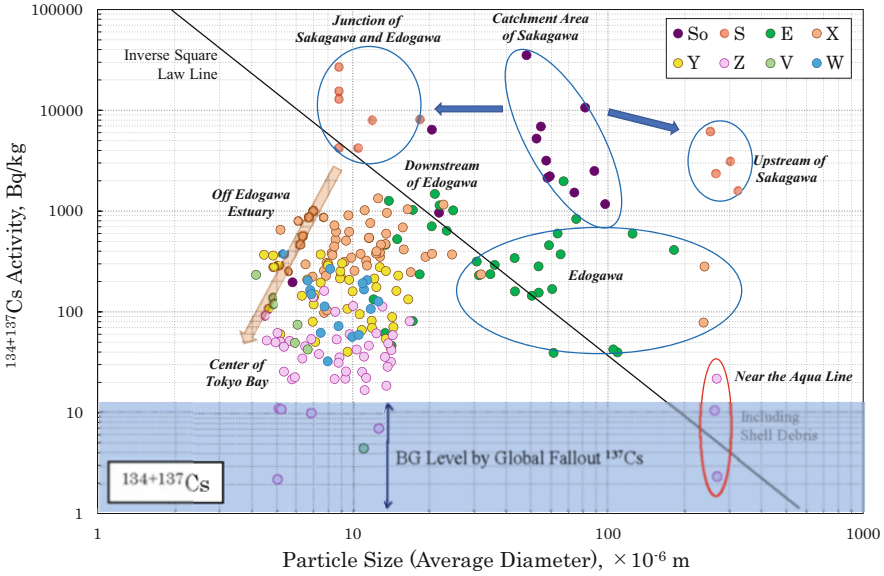

Fig. 6.12 Relationship between the $^{134+137}$Cs activities and the grain size of surface sediments in the Tokyo Bay water system. S_o: Soil in the Sakagawa catchment area, S: Sakagawa River, E: Edogawa and Old Edogawa Rivers, X: Old Edogawa estuary, Y: Offshore the Old Edogawa estuary, Z: Center of Tokyo Bay, V: Tamagawa estuary, W: Sumidagawa estuary. The vertical arrow indicates the range of background ^{137}Cs referred from the JCG report [24]

levels that flowed in from rivers other than the Edogawa water system. The distributions in Area W (estuary of the Sumidagawa River) and Area V (estuary of the Tamagawa River) also support the possibility of dilution effects. This dilution effect is also observed with heavy metals.

Nevertheless, the relationship between cesium radioactivity and particle size in Tokyo Bay is very different from that observed in the estuary of the Abukuma River, which flows through areas most polluted by the FDNPP accident [61–63]. This difference is probably because the Abukuma River estuary faces the Pacific Ocean, where the particle sizes of polluted suspended particles are mixed and separated due to tides and waves. On the other hand, Tokyo Bay is closed, so it is not affected by ocean waves. As a result, large particles contaminated with radioactive cesium preferentially accumulate in the river estuaries as the flow velocity decreases, and small particles are carried to the center of the bay where they settle. Such a mechanism can explain the distribution in Fig. 6.12. The size range of sediments in Area X is 5–30 μm, where the highest concentrations and large amounts of radioactive cesium were deposited in the Old Edogawa estuary. The settling velocity of particles of these sizes is approximately 2–60 m/day, and in a water depth of 5–10 m, contaminated particles can quickly settle to the bottom of the sea well within their residence time [64]. The behavior of radioactive cesium in the Tokyo Bay water system means that the fate of radioactive cesium was determined when it precipitated on the ground surface.

6.9 Balance of Radioactive Cesium Flowing into Tokyo Bay from the Edogawa Watershed

The inventory of $^{134+137}$Cs standardized to March 16, 2011, was estimated for the source and the sink of each area in Fig. 6.13. Table 6.8 shows the balance of radioactive cesium between the Edogawa water system and the Tokyo Bay sediment based on the analytical results. The amount of $^{134+137}$Cs deposited in the Edogawa River basin is estimated to be 8.33 TBq from the results of the MEXT airborne monitoring [1]. Judging from the analytical results of the core samples, the average inventory of $^{134+137}$Cs in Area X, which is 10 km^2 and located approximately 8 km southeast of Chiyoda Ward in central Tokyo, is 131 kBq/m^2 (n = 10). Therefore, the total inventory of $^{134+137}$Cs in this area is 1.31 TBq. Similarly, the average inventory in Area Y is 5.52 kBq/m^2 (n = 11), and the total inventory is 0.22 TBq.

By July 2016, approximately 70% (1.31/1.88 TBq) of radioactive cesium deposited in the study areas has accumulated in Area X. If the amount of deposition in Area Y is included, the total would account for more than 80%. Assuming that the deposited radioactive cesium was all supplied to Area X from the Edogawa River

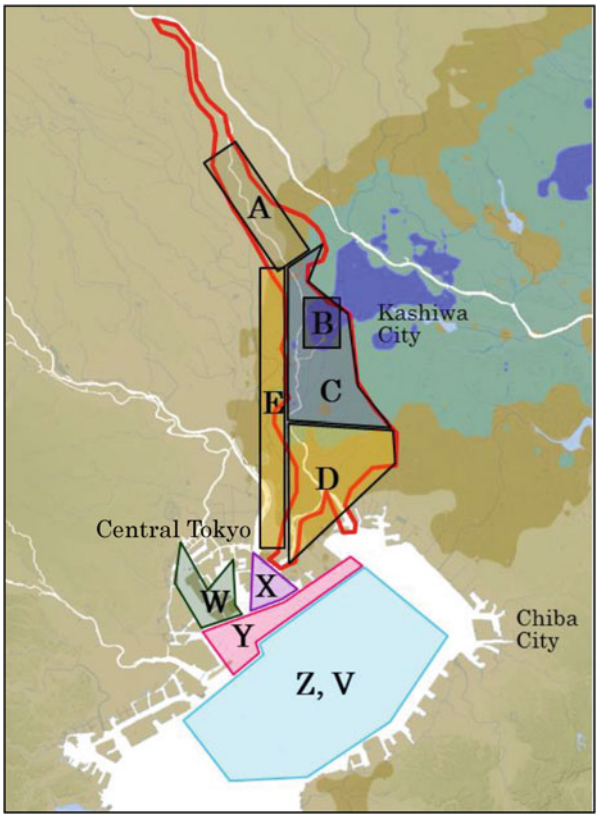

Fig. 6.13 Classification region map for the estimation of radioactive cesium balance in Tokyo Bay and the Edogawa river watershed. The area surrounded by the red line shows the Edogawa river catchment. Area E indicates the Nakagawa river catchment of a branch of the Edogawa river

Table 6.8 Balance of the radioactive cesium precipitated in Tokyo Bay and the Edogawa watershed

	Region[a]		Area, km^2	$^{134+137}Cs$ activity[b]			Ratio to total amount, %
				Inventory, kBq/m^2	Each amount, TBq	Total amount, TBq	
Source[c]	Edogawa Upstream	A	50	10	0.50	**8.33**	
	Kashiwa and Matsudo Cities	B	20	80	1.60		
	Edogawa Midstream	C	65	45	2.93		
	Edogawa Downstream	D	80	20	1.60		
	Nakagawa Watershed	E	85	20	1.70		
Sink[d]	Old-Edogawa Estuary	X	10	131	1.31	**1.53**	**15.7**
	Offshore Area X	Y[e]	40	5.52	0.22		**2.6**
	Central Bay	Z[e], V[e]	330	0.73	0.24	0.24	2.9
	Sumidagawa Estuary	W[e]	20	5.55	0.11	0.11	1.3

[a]Region shows in Fig. 6.13
[b]Decay-corrected value to March 16, 2011
[c]Estimated by the MEXT airborne monitoring [1]
[d]Calculated by the analytical values of the core sediments
[e]Radioactive cesium flowing from rivers other than the Edogawa river system also deposited in these areas

system, approximately 16% (1.31/8.33 TBq) of radioactive cesium precipitated in the catchment area during the 5 years was deposited in Area X after the accident.

On the other hand, it is estimated that critical sources of radioactive cesium for Areas V, W, and Z are other than the Edogawa River system. In particular, in addition to the inflow from the watershed, radioactive plumes from the FDNPP must have precipitated directly onto the sea surface. The inventory for Areas Z and Y in central Tokyo Bay is 0.71–0.80 kBq/m^2, and the cumulative global fallout measured from 1954 to 1995 in Chiba City on the east coast of Tokyo Bay was 6.56 kBq/m^2 [39]. These numbers yield a ratio is equivalent to 11–12%. As shown in Table 5.2, it is estimated that the wastewater treatment system in Tokyo discharged 4.5–12% of the radioactive cesium deposited due to the FDNPP accident. The agreement between these two values for the discharge rate of radioactive cesium from the land is reasonable considering the behavior of the precipitated radioactive cesium.

Since radioactive cesium of 131 kBq/m^2 accumulated in Area X during the 5.4 years after the FDNPP accident, this value represents 20 times the global fallout

of ^{137}Cs. Most of the radioactive cesium flowing into Tokyo Bay was not only contaminated soil from the catchment areas but also contaminated particles that were discharged by decontamination work in highly contaminated zones. As shown in Table 6.7, 0.054 kBq/m^2 day (19.7 kBq/m^2 year) of radioactive cesium is currently flowing into Tokyo Bay via the Old Edogawa River (2016). In other words, most of this radioactive cesium is ^{137}Cs, which has a long half-life of 30.1 years, so for now, the inflow of radioactive cesium of approximately 0.2 TBq/year will continue.

At the southern end of Area W is the unfinished Central Breakwater landfill that is still being reclaimed. Here, sludge incineration ash discharged from the wastewater treatment systems in Tokyo is buried. As described in Table 5.1, the cumulative amount of $^{134+137}$Cs contained in this incinerated ash by the end of 2015 was 0.6 TBq. It must be remembered that radioactive cesium precipitated in urban areas of Tokyo is also transported to Tokyo Bay via such routes and is accumulating.

6.10 Conclusions

Changes in radioactive cesium contamination of Tokyo Bay sediments surrounded by the Tokyo metropolitan area during 5 years after the FDNPP accident are discussed. From August 2011 to July 2016, monitoring surveys were conducted on the spatiotemporal distribution of radioactive cesium released by the FDNPP accident across a 400 km^2 area in the northern part of Tokyo Bay and its incoming rivers. Most of the radioactive cesium flowed from highly contaminated areas in the northeastern Tokyo metropolitan area through the Old Edogawa River into Tokyo Bay and accumulated off the estuary without spreading to the center of the bay. The $^{134+137}$Cs concentration increased immediately after the accident, peaked at the end of 2012 at 556 Bq/kg, and then decreased according to radioactive decay. However, the inventory of $^{134+137}$Cs offshore from the Old Edogawa estuary increased to 104 kBq/m^2 in July 2016. At this time, approximately 70% of the radioactive cesium accumulated in the Tokyo Bay sediment was deposited in sediments of Area X in the Old Edogawa estuary.

On the other hand, the concentration of $^{134+137}$Cs in sediments of the central part (Area Z) of Tokyo Bay was 17 $\pm$ 0.3 kBq/kg (weighted average, n = 50). Most likely, radioactive cesium was transported to Tokyo Bay as contaminated soil particles from highly polluted areas in the northeastern Tokyo metropolitan area through rivers such as the Sakagawa, Edogawa, and Old Edogawa rivers. Observation results suggest that rivers play an essential role in transporting radioactive cesium from land sources. Additionally, radioactive cesium precipitated from the atmosphere and adsorbed on soil particles enters the rivers as polluted particles but selectively settles and accumulates at the estuaries around Tokyo Bay, where the flow velocity of the river water decreases. Therefore, it is estimated that radioactive cesium has not spread to the center of the bay. The flux of $^{134+137}$Cs offshore of the Old Edogawa estuary decreased sharply immediately after the accident, but afterward, it mostly agreed with the value predicted based on radioactive decay.

Conversely, the inventory in sediments is increasing. The average flux from 2014 to 2016 was approximately 0.055 kBq/m^2. It is calculated that 8.33 TBq of $^{134+137}$Cs was deposited in the basin of the Edogawa water system and that 1.53 TBq of these radionuclides migrated through the river and was deposited in the estuary of the Old Edogawa river by July 2016. Currently, approximately 0.2 TBq of radioactive cesium per year continues to flow into the inner part of Tokyo Bay. The radioactive cesium that has flowed into Tokyo Bay is retained firmly in its sediments, so Tokyo Bay plays an essential role as a reservoir of radioactive cesium discharged from the Tokyo metropolitan area.

References

1. MEXT (Ministry of Education, Culture, Sports, Science and Technology of Japan) (2011) MEXT's airborne monitoring results in Iwate, Shizuoka, Nagano, Yamanashi, Gifu, and Toyama prefectures and revisions to airborne monitoring that take into account the effects of natural nuclides [in Japanese]. https://radioactivity.nsr.go.jp/ja/contents/5000/4899/24/1910_111112nd.pdf
2. Yamazaki H, Ishida M, Hinokio R, Yamashiki YA, Azuma R (2018) Spatiotemporal distribution and fluctuation of radiocesium in Tokyo Bay in the five years following the Fukushima Daiichi Nuclear Power Plant (FDNPP) accident. PLoS One 13:e0193414. https://doi.org/10.1371/journal.pone.0193414
3. MOE (Ministry of Environment, Japan) (2009) Enclosed coastal seas in Japan (88 areas). Environmental Guidebook [in Japanese]. https://www.env.go.jp/water/heisa/heisa_net/downloadData/Guidebook/guidebook00.pdf. International EMECS Center [in English]. http://www.emecs.or.jp/en/encsea
4. MLIT (Ministry of Land, Infrastructure, Transport and Tourism of Japan) (2014) Water environment in Tokyo Bay [in Japanese]. https://www1.kaiho.milt.go.jp/KANKYO/TB_Renaissane/RenaissanceProject/Handouts/7th/H03.pdf
5. MLIT (2014) Overview of Tokyo Bay and the catchment area [in Japanese]. https://www.ktr.mlit.go.jp/ktr_content/000621812.pdf
6. Guo X, Yanagi T (1994) Three dimensional structure of tidal currents in Tokyo Bay, Japan. La mer 32:173–185
7. Kakehi S, Kaeriyama H, Ambe D, Ono T, Ito S et al (2016) Radioactive cesium dynamics derived from hydrographic observations in the Abukuma River Estuary, Japan. Environ Radioact 153:1–9. https://doi.org/10.1016/j.jenvrad.2015.11.015
8. Yamasaki S, Imoto J, Furuki G, Ochiai A, Ohnuki T et al (2016) Radioactive Cs in the estuary sediments near Fukushima Daiichi Nuclear Power Plant. Sci Total Environ 551-552:155–162. https://doi.org/10.1016/j.scitotenv.2016.01.155
9. Saegusa H, Ohyama T, Iijima K, Onoe H, Takeuchi R et al (2016) Deposition of radiocesium on the river flood plains around Fukushima. J Environ Radioact 164:36–46. https://doi.org/10.1016/j.jenvrad.2016.04.020
10. Tsuruta H, Nakajima T (2012) Radioactive materials in the atmosphere released by the accident of the Fukushima Daiichi Nuclear Power Plant. Chikyukagaku (Geochemistry) 46:99–111. [in Japanese with English abstract]. https://doi.org/10.14934/chikyukagaku.46.99
11. Ishida M, Yamazaki H (2017) Radioactive contamination in the Tokyo metropolitan area in the early stage of the Fukushima Daiichi Nuclear Power Plant (FDNPP) accident and its fluctuation over five years. PLoS One 12:e0187687. https://doi.org/10.1371/journal.pone.0187687
12. USNRC (US Nuclear Regulatory Commission) (1989) Programmatic Environmental Impact Statement related to decontamination and disposal of radioactive wastes resulting from March

28, 1979 accident Three Mile Island Nuclear Station, Unit 2. https://ntrl.ntis.gov/NTRL/dashboard/searchResults/titleDetail/NUREG0683SUPN3.xhtml
13. NSAC (Nuclear Science Advisory Committee) (1980) Analysis of Three Mile Island-Unit 2 accident. NSAC-80-1. http://www.iaea.org/inis/collection/NCLCollectionStore/_Public/13/677/13677904.pdf
14. IAEA (International Atomic Energy Agency) (2006) Environmental consequences of the Chernobyl accident and their remediation: twenty years of experience. Report of Chernobyl Forum Expert Group 'Environment'. IAEA Radiological Assessment Reports Series. https://www-pub.iaea.org/MTCD/publications/PDF/Pub1239_web.pdf
15. Saito-Kokubu Y, Yasuda K, Magara M, Miyamoto Y, Sakurai S et al (2007) Geographical distribution of plutonium derived from the atomic bomb in the eastern area of Nagasaki. J Radioanal Nucl Chem 273:183–186. https://doi.org/10.1007/s10967-007-0733-9
16. Saito-Kokubu Y, Esaka F, Yasuda K, Magara M, Miyamoto Y et al (2007) Plutonium isotopes derived from Nagasaki atomic bomb in the sediment of Nishiyama reservoir at Nagasaki, Japan. Int J Appl Radiat Isotopes 65:465–468. https://doi.org/10.1016/j.apradiso.2006.10.010
17. Saito-Kokubu Y, Yasuda K, Magara M, Miyamoto Y, Sakurai S et al (2008) Depositional records of plutonium and ^{137}Cs released from Nagasaki atomic bomb in sediment of Nishiyama reservoir at Nagasaki. J Environ Radioact 99:211–217. https://doi.org/10.1016/j.jenvrad.2007.11.010
18. Gallego E (2006) MUD; a model to investigate the migration of ^{137}Cs in the urban environment and drainage and sewage treatment systems. J Environ Radioact 85:247–264. https://doi.org/10.1016/j.jenvrad.2004.10.017
19. Pratama MA, Yoneda M, Yamashiki Y, Shimada Y, Matsui Y (2014) Modeling migration of Cs-137 in sewer system of Fukushima City using urban environment and drainage system (MUD). Int J Eng Tech 6:402–408. https://doi.org/10.7763/IJET.2014V6.732
20. USGS (US Geological Survey) (1973) Distribution of radionuclides in bottom sediments of the Columbia River estuary. Geological Survey Professional Paper 433-1. https://pubs.usgs.gov/pp/0433l/report.pdf
21. USCS (1975) Distribution of radionuclides in the Columbia River streambed, Hanford reservation to Longview, Washington. Geological Survey Professional Paper 433-O. https://pubs.usgs.gov/pp/0433l/report.pdf
22. Bera G, Yeager KM, Shim M, Shiller AM (2015) Anthropogenic stable cesium in water and sediment of a shallow estuary, St. Louis Bay, Mississippi. Estuar Coast Shelf Sci 157:32–41. https://doi.org/10.1016/j.ecss.2015.02.004
23. NRA (Nuclear Regulation Authority, Japan) (2013) Readings of Sea Water at Tokyo Bay. http://radioactivity.nsr.go.jp/en/list/290/list-1.html
24. JCG (Japan Coast Guard) (2016) Report of Radioactivity Surveys. Results of Surveys in 2016 [in Japanese]. http://www1.kaiho.mlit.go.jp/KANKYO/OSEN/housha.html
25. Koibuchi Y (2013) Tracing fine-grained sediment transport around Tokyo Bay using cesium-134 and cesium-137 originating from Fukushima Daiichi Power Plant. In: Rodriguez GR (ed) Coastal processes III. WIT Press, Southampton, pp 191–201. https://doi.org/10.2495/CP130171
26. Aoyama M, Hirose K (2008) Analysis of environmental radionuclides. In: Povinec PP (ed) Radiometric determination of anthropogenic radionuclides in seawater. Elsevier, London, pp 137–162. https://doi.org/10.1016/S1569-4860(07)11004-4
27. Yasuhara M, Yamazaki H (2005) The impact of 150 years of anthropogenic pollution on the shallow marine ostracode fauna, Osaka Bay, Japan. Mar Micropaleontol 55:63–74. https://doi.org/10.1016/j.marmicro.2005.02.005
28. Gohda S, Yamazaki H, Hirata M, Nagasawa T (1987) XRF analysis of rock and sediment using standard rock samples. BUNSEKI KAGAKU (Analytical Chemistry) 36:199–203. [in Japanese with English abstract]
29. Oikawa S, Watabe T, Takata H, Suzuki C, Nakahara M et al (2013) Long term temporal changes of ^{90}Sr and ^{137}Cs in sea water, bottom sediment and marine organism samples – from

the Chernobyl accident to immediately after the Fukushima accident. BUNSEKI KAGAKU (Analytical Chemistry) 62:455–474. [in Japanese with English abstract]. https://doi.org/10.2116/bunsekikagaku.62.455
30. Chaisan K, Smith JT, Bossew P, Kirchner G, Loptev GV (2013) Worldwide isotope ratios of the Fukushima release and early-phase external dose reconstruction. Sci Rep 3:2520. https://doi.org/10.1038/srep02520
31. Komori M, Shozugawa K, Nogawa N, Matsuo M (2013) Evaluation of radioactive contamination caused by each plant of Fukushima Daiichi Nuclear Power Station using $^{134}Cs/^{137}Cs$ activity ratio as an index. BUNSEKI KAGAKU (Analytical Chemistry) 62:475–483. [in Japanese with English abstract]. https://doi.org/10.2116/bunsekikagaku.62.475
32. Nishizawa Y, Yoshida M, Sanada Y, Torii T (2016) Distribution of the $^{134}Cs/^{137}Cs$ ratio around the Fukushima Daiichi nuclear power plant using an unmanned helicopter radiation monitoring system. J Nucl Sci Technol 53:468–474. https://doi.org/10.1080/00223131.2015.1071721
33. Sekiguchi H, Yamazaki H, Nakagawa R, Ishida M, Azuma R et al (2013) Implications of flood event layers in littoral sedimentary environments. J JSCE, Ser B2. Coast Eng 69:691–695. [in Japanese with English abstract]
34. Kashiwa City Government (2013) Decontamination project in Kashiwa City, 2nd edn. [in Japanese]. http://www.city.kashiwa.lg.jp/houshasenkanren/3331/3332/p032036_d/fil/jissikeikaku250613.pdf
35. Japan Meteorological Agency (2020) Search past weather data [in Japanese]. https://www.data.jma.go.jp/obd/stats/etrn/select/prefecture00
36. MLIT. Edogawa River Office (2015) River Management Report 2015 [in Japanese]. http://www.ktr.mlit.go.jp/ktr_content/content/000642546.pdf
37. MLIT (2015) Overview of the Kanto-Tohoku heavy rainfall disaster [in Japanese]. http://www.bousai.go.jp/fusuigai/suigaiworking/pdf/dai1kai/siryo1.pdf
38. Yamada M, Nagaya Y (2000) $^{239+240}Pu$ and ^{137}Cs in sediments from Tokyo Bay: distribution and inventory. J Radioanal Nucl Chem 245:273–279. https://doi.org/10.1023/A:1006741917854
39. JCAC (Japan Chemical Analysis Center). Radioactivity survey data in Japan. Environmental and dietary materials. http://www.kankyo-hoshano.go.jp/en/07/07.html
40. Håkanson L (2004) Modelling the transport of radionuclides from land to water. J Environ Radioact 73:267–287. https://doi.org/10.1016/j.jenvrad.2003.10.003
41. Håkanson L (2004) A new generic sub-model for radionuclide fixation in large catchments from continuous and single-pulse fallouts, as used in a river model. J Environ Radioact 77:247–273. https://doi.org/10.1016/j.jenvrad.2004.03.010
42. Smith JT, Wright SM, Cross MA, Monte L, Kudelsky AV et al (2004) Global analysis of the riverine transport of ^{90}Sr and ^{137}Cs. Environ Sci Technol 38:850–857. https://doi.org/10.1021/es0300463
43. Monte L, Boyer P, Brittain JE, Håkanson L, Lepicard S et al (2005) Review and assessment of models for predicting the migration of radionuclides through rivers. J Environ Radioact 79:273–296. https://doi.org/10.1016/j.jenvrad.2004.08.002
44. Förstner U (1983) Metal transfer between solid and aqueous phases. In: Förstner U, Wittmann GTW (eds) Metal pollution in the aquatic environment. Springer, New York, NY, pp 247–270
45. Stumm W, Morgan JJ (1996) The solid-solution interface. In: Stumm W, Morgan JJ (eds) Aquatic chemistry, 3rd edn. John Wiley & Sons, New York, NY, pp 516–608
46. Sawhney BL (1972) Selective sorption and fixation of cations by clay minerals: a review. Clay Clay Miner 20:93–100. https://doi.org/10.1346/CCMN.19720200208
47. Evans DW, Alberts JJ, Clark RA III (1983) Reversible ion-exchange fixation of cesium-137 leading to mobilization from reservoir sediments. Geochim Cosmochim Acta 47:1041–1049. https://doi.org/10.1016/0016-7037(83)90234-X
48. Bostick BC, Vairavamurthy MA, Karthikeyan KG, Chorover J (2002) Cesium adsorption on clay minerals: an EXAFS spectroscopic investigation. Environ Sci Technol 36:2670–2676. https://doi.org/10.1021/es0156892

49. Zachara JM, Smith SC, Liu C, McKinley JP, Serne RJ et al (2002) Sorption of Cs^+ to micaceous subsurface sediments from the Hanford site, USA. Geochim Cosmochim Acta 66:193–211. https://doi.org/10.1016/S0016-7037(01)00759-1
50. Qin H, Yokoyama Y, Fan Q, Iwatani H, Tanaka K, Sakaguchi A et al (2012) Investigation of cesium adsorption on soil and sediment samples from Fukushima Prefecture by sequential extraction and EXAFS technique. Geochem J 46:297–302. https://doi.org/10.2343/geochemj.2.0214
51. Motokawa R, Endo H, Yokoyama S, Nishitsuji S, Kodayashi T et al (2014) Collective structural changes in vermiculite clay suspensions induced by cesium ions. Sci Rep 4:6585. https://doi.org/10.1038/srep06585
52. Tokuda Y, Norikawa Y, Masai H, Ueda Y, Nihei N et al (2016) Nuclear magnetic resonance study of Cs adsorption onto clay minerals. Radio Issu Fukushima's Revital Fut 1:3–11. https://doi.org/10.1007/978-4-431-55848-4_1
53. Adachi K, Kajino M, Zaizen Y, Igarashi Y (2013) Emission of spherical cesium-bearing particles from an early stage of the Fukushima nuclear accident. Sci Rep 3:2554. https://doi.org/10.1038/srep02554
54. Itoh S, Eguchi T, Kato N, Takahashi S (2014) Radioactive particles in soil, plant, and dust samples after the Fukushima nuclear accident. Soil Sci Plant Nutr 60:440–550. https://doi.org/10.1080/00380768.2014.907735
55. Abe Y, Iizawa Y, Terada Y, Adachi K, Igarashi Y, el al. (2014) Detection of uranium and chemical state analysis of individual radioactive microparticles emitted from the Fukushima nuclear accident using multiple synchrotron radiation X-ray analysis. Anal Chem 86:8521–8525. https://doi.org/10.1021/ac501998d
56. Yamaguchi N, Mitome M, Kotone H, Asano M, Adachi K et al (2016) Internal structure of cesium-bearing radioactive microparticles released from Fukushima nuclear power plant. Sci Rep 6:20548. https://doi.org/10.1038/srep20548
57. Furuki G, Imoto J, Ochiai A, Yamasaki S, Nanba K et al (2017) Caesium-rich micro-particles: a window into the meltdown events at the Fukushima Daiichi Nuclear Power Plant. Sci Rep 7:42731. https://doi.org/10.1038/srep42731
58. Stumm W, Morgan JJ (1996) Particle-particle interaction: colloids, coagulation, and filtration. In: Stumm W, Morgan JJ (eds) Aquatic chemistry, 3rd edn. John Wiley & Sons, New York, NY, pp 818–871
59. Thill A, Mousteir S, Garnier JM, Estournel C, Naudin JJ et al (2001) Evolution of particle size and concentration in Rhône river mixing zone: influence of salt flocculation. Cont Shelf Res 21:2127–2140. https://doi.org/10.1016/S0278-4343(01)00047-4
60. Förstner U (1983) Grain-size effects. In: Förstner U, Wittmann GTW (eds) Metal pollution in the aquatic environment. Springer, New York, NY, pp 121–132
61. Yamashiki Y, Onda Y, Smith HG, Blake WH, Wakahara T et al (2013) Initial flux of sediment-associated radiocesium to the ocean from the largest river impacted by Fukushima Daiichi Nuclear Power Plant. Sci Rep 4:3714. https://doi.org/10.1038/srep03714
62. Tanaka K, Iwatani H, Sakaguchi A, Fan Q, Takahashi Y (2015) Size-dependent distribution of radiocesium in riverbed sediments and its relevance to the migration of radiocesium in river systems after the Fukushima Daiichi Nuclear Power Plant accident. J Environ Radioact 139:390–397. https://doi.org/10.1016/j.jenvrad.2014.05.002
63. Pratama M, Yoneda M, Shimada Y, Matsui Y, Yamashiki Y (2015) Future projection of radiocesium flux to the ocean from the largest river impacted by Fukushima Daiichi Nuclear Power Plant. Sci Rep 5:8408. https://doi.org/10.1038/srep08408
64. Wada A, Takano T, Hoizumi T (1994) Estimation of bay-water retention time. Ann J Hydr Eng, B1, JSCE 34:331–336. [in Japanese with English Abstract]